Mobile DNA

RESEARCH

Open Access

A T cell receptor specific for an HLA-A*03:01-restricted epitope in the endogenous retrovirus ERV-K-Env exhibits limited recognition of its cognate epitope

Erin E. Grundy[1,2,3], Lauren C. Shaw[4], Loretta Wang[1,2], Abigail V. Lee[1,2,3], James Castro Argueta[5], Daniel J. Powell Jr[4], Mario Ostrowski[6], R. Brad Jones[7], C. Russell Y. Cruz[2,3,8], Heather Gordish-Dressman[5,9], Nicole P. Chappell[2], Catherine M. Bollard[2,3,8] and Katherine B. Chiappinelli[1,2,3*]

Abstract

Transposable elements (TEs) are often expressed at higher levels in tumor cells than normal cells, implicating these genomic regions as an untapped pool of tumor-associated antigens. In ovarian cancer (OC), protein from the TE ERV-K is frequently expressed by tumor cells. Here we determined whether the targeting of previously identified epitope in the envelope gene (*env*) of ERV-K resulted in target antigen specificity against cancer cells. We found that transducing healthy donor T cells with an ERV-K-Env-specific T cell receptor construct resulted in antigen specificity only when co-cultured with HLA-A*03:01 B lymphoblastoid cells. Furthermore, in vitro priming of several healthy donors with this epitope of ERV-K-Env did not result in target antigen specificity. These data suggest that the T cell receptor is a poor candidate for targeting this specific ERV-K-Env epitope and has limited potential as a T cell therapy for OC.

Keywords Tumor immunology, Immunotherapy, Transposable elements, Endogenous retroviruses, T cell receptor

*Correspondence:
Katherine B. Chiappinelli
kchiapp1@email.gwu.edu
[1] Department of Microbiology, Immunology and Tropical Medicine, The George Washington University, Washington, DC, USA
[2] The George Washington University Cancer Center, Washington, DC, USA
[3] The Integrated Biomedical Sciences at the George Washington University, Washington, DC, USA
[4] Department of Pathology and Laboratory Medicine, Center for Cellular Immunotherapies, Perelman School of Medicine, Ovarian Cancer Research Center, The University of Pennsylvania, Philadelphia, PA, USA
[5] The George Washington School of Medicine and Health Sciences, The George Washington University, Washington, DC, USA
[6] Department of Medicine, University of Toronto, Toronto, Canada
[7] Weill Cornell Medicine Graduate School of Medical Sciences, New York, NY, USA
[8] Center for Cancer and Immunology, , Children's National Hospital, Washington, DC, United States
[9] The Center for Translational Research, Children's National Hospital, Washington, DC, USA

Background

Due to the lack of reliable early detection methods for ovarian cancer (OC), patients with this disease are typically diagnosed at late stages. Combined with the lack of effective therapies, patients often succumb to this malignancy [1, 2]. Unlike the dramatic responses to immunotherapy seen with more immunogenic cancer types, such as melanoma and non-small cell lung cancer, OC is less responsive to immune checkpoint blockade, achieving a maximum overall response rate of 31% lasting less than 4 months [3–14]. While OC does not respond well to immunotherapy, treatment of OC tumor cells with epigenetic drugs stimulates an anti-tumor interferon immune signaling response in in vitro and murine models of OC [15–17]. Treating OC cells with DNA methyltransferase inhibitors or histone deacetylase inhibitors induces the

expression of transposable elements (TEs)—genomic regions that are epigenetically silenced in healthy cells to prevent their mobility and destabilization of the genome [18] [19]. As the structure of some transcribed TEs resembles that of viral nucleic acids, their expression stimulates type I and III interferon signaling pathways in tumor cells in a process termed "viral mimicry" [15, 20, 21]. Treatment of tumor cells with epigenetic inhibitors also increases the expression of antigen processing and presentation machinery, rendering tumor cells more visible to the immune system [22]. Combining the increased expression of TEs in tumor cells in response to epigenetic therapy with enhanced antigen presentation implicates their use as potential targetable tumor-associated antigens.

A higher number of intratumoral T cells is positively correlated with higher overall survival in patients with OC, implying that the presence of T cells within the tumor is positively associated with disease control [23, 24]. While OC development is driven by genomic rearrangements, it has a relatively low mutational burden, with few neoantigens present [5, 25, 26]. One reason that patients with OC who have higher numbers of intratumoral T cells experience longer overall survival rates may be that these intratumoral T cells recognize non-conventional antigens, derived from TEs. One class of TEs frequently overexpressed in OC are long terminal repeat elements, particularly endogenous retroviruses (ERVs) [27–29]. ERVs are the remnants of viruses that have integrated into the human germline millions of years ago [30, 31]. ERVs are composed of three genes—*gag*, *pol,* and *env*—with a long terminal repeat flanking the genes. Proteins derived from the *gag* and *env* genes of the ERV-K family are frequently expressed/overexpressed in several types of cancers, including OC [27, 32–37].

Previous work has shown that protein derived from the entire envelope gene of the ERV-K(HML-2) group (ERV-K-Env) is immunogenic in T cells expanded from peripheral blood mononuclear cells (PBMCs) derived from patients with OC [29]. Separately, a CD8 + T cell clone that recognizes an epitope derived from ERV-K-Env has been isolated from an individual infected with human immunodeficiency virus-1 (HIV-1) [38]. T cells harboring a T cell receptor (TCR) for this epitope were able to recognize and kill HIV-1-infected cells. The minimal epitope recognized by this clone was mapped to an HLA-A*03:01-restricted epitope of ERV-K-Env that is 12 – 15 amino acids in length. This peptide spans amino acids 413 – 427 of the *env* gene, placing it in the surface domain [39] [40]. As HLA I (human equivalent of major histocompatibility complex I/MHC I) canonically presents epitopes that are 8 – 11 amino acids in length, a 12 – 15 amino acid peptide is unusually long for HLA I to present to CD8 + T cells [41] [42]. However, this ERV-K-Env-specific T cell clone eliminated HLA-matched CD4 + T cells infected with HIV-1. For this study, we aimed to determine whether this HLA-A*03:01-restricted TCR clone could recognize its cognate epitope outside the HIV-1 setting, with the goal of using it as an immunogenic OC target. Some populations in the United States have up to 6% HLA-A*03:01 positivity [43]. In this work, we used IFN-γ enzyme-linked immunosorbent spot (ELISpot) assays and intracellular cytokine staining to determine that T cells transduced with the ERV-K-Env-specific TCR only responded to the cognate peptide when presented by HLA-A*03:01 B lymphoblastoid cells from multiple donors, but not HLA-A*03:01 OC cells or HLA-matched antigen presenting cells. We also did not observe specificity towards this epitope from in vitro primed T cells expanded from healthy donors. Together, our findings demonstrate that this TCR is not a good candidate for targeting this epitope of ERV-K-Env.

Results

Lack of specificity of the ERV-K-Env-specific TCR against OC cell lines

The HLA-A*03:01-restricted ERV-K-Env-specific TCR was first identified in an individual positive for HIV-1, donor OM9 [38]. The epitope sequence of ERV-K-Env that the TCR recognizes is shown in Figure S1a. The minimal epitope is 12 amino acids in length, which is unusually long for MHC class I [42]. The longer epitope (the 15mer) is identical to the 12mer with 3 additional amino acids at the C-terminus end of the epitope. Hereafter, the epitopes are referred to together as ERV-K-Env. The first plasmid construct of this TCR (construct OM9.1), yielded low transduction efficiency in T cells isolated from several healthy donors (average ~ 12.1% ± 9.1%) (Figure S1b-d). The construct was optimized (construct OM9.2) by cloning the TCR into a lentiviral vector under the control of the EF-1α promoter (Figure S2a-b). To confirm that the TCR was being expressed on the cell surface, SupT1 cells—which lack an endogenously expressed TCR on their surface—were transduced with the OM9.2 construct and analyzed for CD3 and TCR-α/β expression via flow cytometry (Figure S2c). Following this validation, GFP expression was used to confirm the transduction efficiency of donors in subsequent experiments. The OM9.2 construct yielded an average transduction efficiency of ~ 83.9% ± 12.5% in T cells isolated from multiple healthy donors (Figure S2d), indicating that primary T cells can be efficiently transduced to express the TCR.

To test whether OM9.2-expressing T cells specifically recognized HLA-A*03:01 OC cells at an increased level compared to unmodified T cells, we used the enzyme-linked immunosorbent spot (ELISpot) assay to detect

interferon-γ (IFN-γ) secretion from T cells in the presence of antigen (Fig. 1a). Both untransduced (control) and OM9.2 T cells had low background secretion of IFN-γ when cultured in the absence of any antigen or with a negative control peptide (Fig. 1b-c, "media" and "actin", respectively; p-values for all TCR experiments are in Tables S1 and S2). There was no significant difference in the amount of IFN-γ secreted by OM9.2 T cells compared to untransduced T cells plated with HLA-A*03:01 OC cell lines ES-2 and TOV112D at any effector:target ratio tested (Fig. 1b-c, "ES-2" and "TOV112D"). However, both OM9.2 T cells and untransduced T cells were immunologically functional as they were both capable of secreting large amounts of IFN-γ in the presence of the mitogen phytohemagglutinin (PHA), which stimulates T cells independent of TCR specificity [44] (Fig. 1b-c, "PHA").These data indicate that expression of the HLA-A*03:01-restricted ERV-K-Env-specific TCR does not enable OM9.2 T cells to specifically recognize HLA-A*03:01 OC cells at a higher level compared to untransduced T cells.

ERV-K-Env epitope-specific OM9.2 T cells were not activated by the free ERV-K-Env peptide

To determine whether OM9.2-expressing T cells were capable of responding to the cognate 12mer/15mer peptide of ERV-K-Env when dissolved freely in solution, we repeated the ELISpot assay with T cells and free ERV-K-Env peptide (Fig. 2a). In general, nanogram amounts of peptide are used to test for antigen specificity of T cells in ELISpot assays [45–48]. However, the original reported functional testing of this TCR was performed

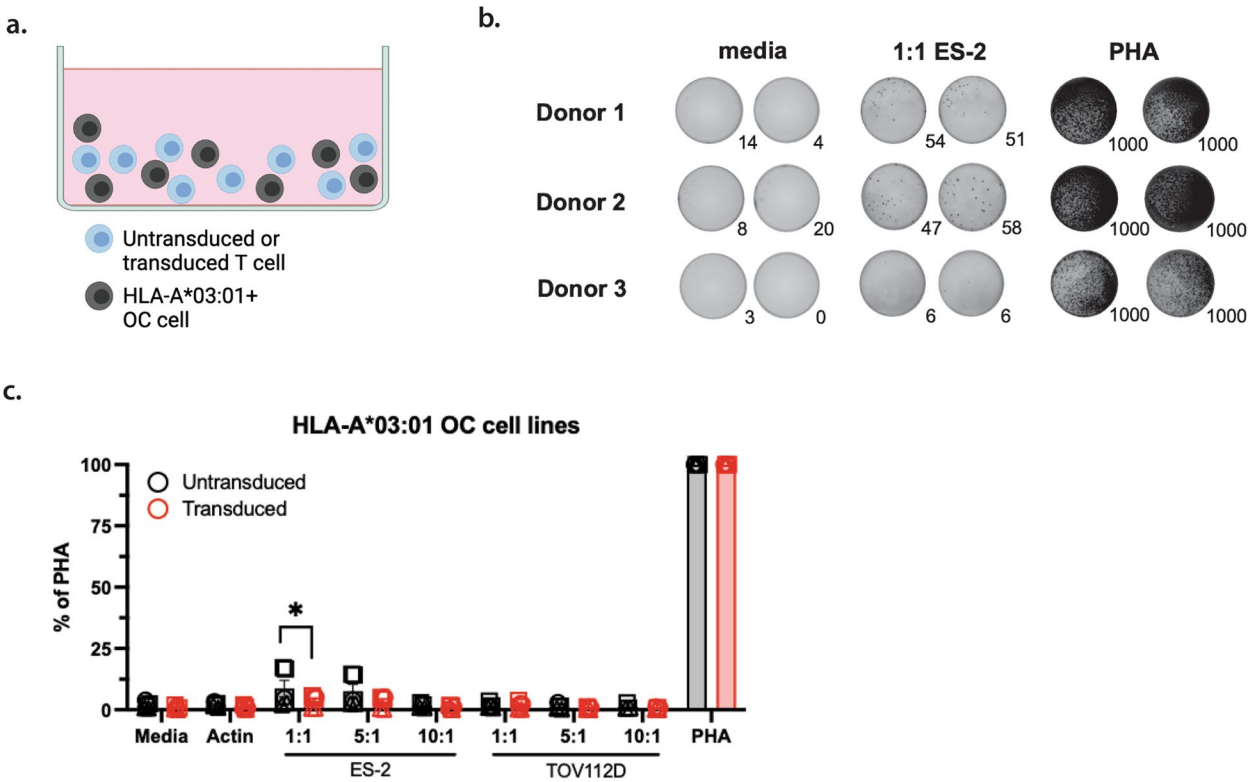

Fig. 1 Lack of specificity of the ERV-K-Env-specific TCR against OC cell lines. **a**. Diagram of the ELISpot assay design used in **b-c**. **b**. Representative images of developed wells for the level of background IFN-γ secretion (media), IFN-γ secretion in the presence of ES-2 cells (1:1 ES-2), and positive control of IFN-γ (PHA) for the ELISpot assay quantified in **c**. Number of spots in each well are indicated to the bottom right of each image. Images shown are for OM9.2 T cells. **c**. Number of IFN-γ spots per well normalized to the positive control (expressed as % of PHA) of untransduced T cells (black) and OM9.2 T cells (red) for the indicated conditions: media = background level of IFN-γ secretion from T cells, actin = negative control, various effector:target ratios of T cells (effectors) with HLA-A*03:01 OC cell lines (targets), PHA = positive control. Each donor is indicated by a different symbol. ELISpot conditions were plated in duplicate or triplicate as cell numbers allowed for $n = 3$ donors. Error bars represent SEM of all data points for all donors. The Wilcoxon rank sum test was used to compare the number of IFN-γ spots between untransduced and transduced T cells (indicated by *). The Kruskal Wallis test was used to compare the number of IFN-γ spots between each antigen condition for a given T cell type. Any Kruskal Wallis test that had $p < 0.05$ was followed by post-hoc pairwise Wilcoxon rank sum tests and adjusted for multiple comparisons (indicated by #). All statistical comparisons for TCR experiments are in Tables S1 and S2. *$p < 0.05$, **$p < 0.005$, ***$p < 0.0005$. ELISpot = Enzyme-linked immunosorbent spot; PHA = phytohemagglutinin; OC = ovarian cancer; SEM = standard error of the mean

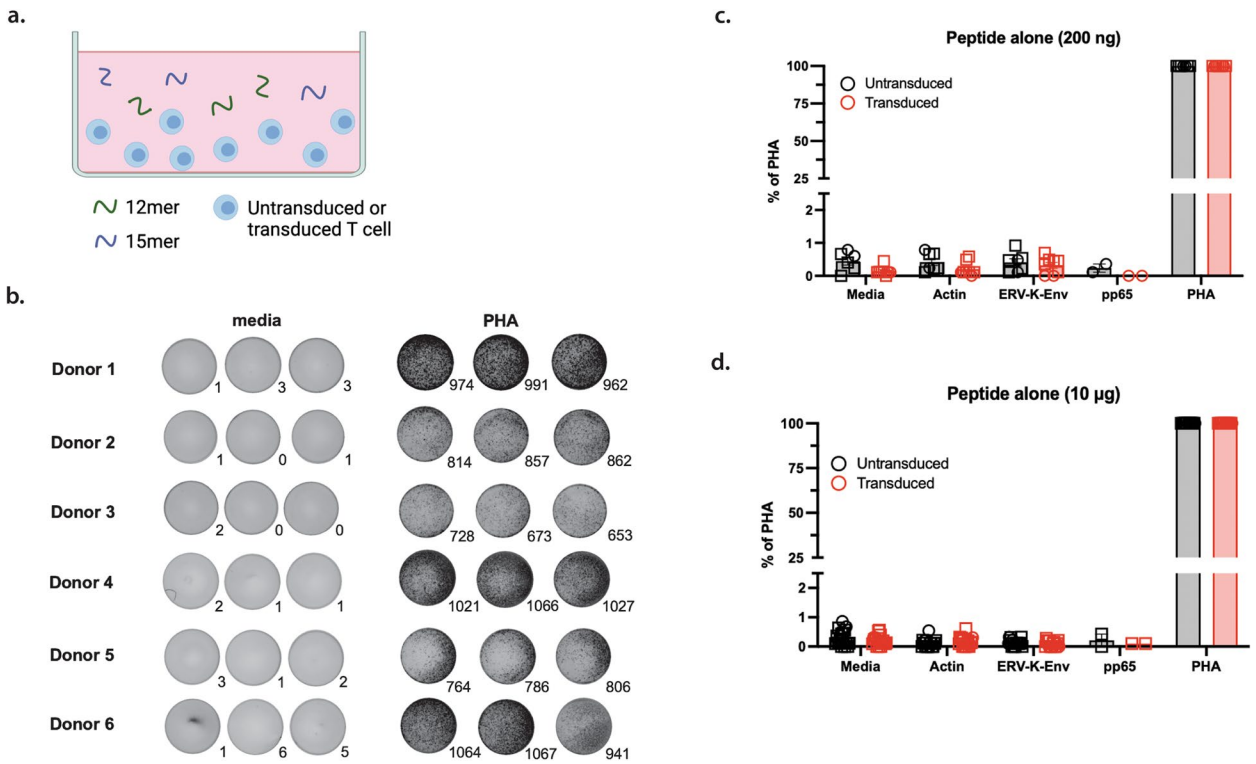

Fig. 2 OM9.2 T cells were not activated by free ERV-K-Env peptide. **a**. Diagram of the ELISpot assay design used in **b-d**. **b**. Representative images of developed wells for the level of background IFN-γ secretion (media) and positive control of IFN-γ (PHA) for the ELISpot assays quantified in **c-d**. Number of spots in each well are indicated to the bottom right of each image. Images shown are for OM9.2 T cells. **c-d**. Number of IFN-γ spots per well normalized to the positive control (expressed as % of PHA) of untransduced T cells (black) and OM9.2 T cells (red) for the indicated conditions: media = background level of IFN-γ secretion from T cells, actin = negative control, ERV-K-Env = ERV-K-Env epitope, pp65 = HLA-B*35 off-target control, PHA = positive control. Each donor is indicated by a different symbol. ELISpot conditions were plated with the indicated peptide concentrations in duplicate or triplicate as cell numbers allowed at 200 ng for $n = 2$ donors (**c**) or at 10 µg for $n = 6$ donors (**d**). Error bars represent SEM of all data points for all donors. The Wilcoxon rank sum test was used to compare the number of IFN-γ spots between untransduced and transduced T cells (indicated by *). The Kruskal Wallis test was used to compare the number of IFN-γ spots between each antigen condition for a given T cell type. Any Kruskal Wallis test that had $p < 0.05$ was followed by post-hoc pairwise Wilcoxon rank sum tests and adjusted for multiple comparisons (indicated by #). All statistical comparisons for TCR experiments are in Tables S1 and S2. *$p < 0.05$, **$p < 0.005$, ***$p < 0.0005$. ELISpot = Enzyme-linked immunosorbent spot; PHA = phytohemagglutinin; SEM = standard error of the mean

using relatively high concentrations of peptide, in the tens of micrograms range [38]. Therefore, we tested both a low concentration of peptide (200 ng per well, Fig. 2c) and a high concentration of peptide (10 µg per well, Fig. 2d). Again, both OM9.2 T cells and untransduced T cells from $n = 6$ donors had low background secretion of IFN-γ when cultured in the absence any antigen or with low or high concentrations of the negative control peptide actin (Fig. 2c-d). As an additional control, neither OM9.2 T cells nor untransduced T cells from donors 1 and 2 secreted IFN-γ in response to a low or high concentration of an HLA-mismatched off-target control peptide from pp65 (Fig. 2c-d). The epitope of pp65 used here is an HLA-B*35-restricted peptide from cytomegalovirus as Donors 1–6 were HLA-B*35-negative (Table S3). OM9.2 T cells were not capable of responding to a low or high concentration of the ERV-K-Env peptide as there was no significant difference in IFN-γ secretion in the presence of antigen compared to untransduced T cells (Fig. 2c-d). Again, all T cells were immunologically functional as they secreted IFN-γ in the presence of PHA. These data indicate that OM9.2 T cells are not capable of recognizing free ERV-K-Env peptide in solution, which led us to hypothesize that the affinity of the OM9.2 TCR for the cognate peptide-MHC complex was low.

ERV-K-Env epitope-specific OM9.2 T cells were not activated by the ERV-K-Env peptide when presented by peptide-pulsed APCs

While tetramer staining would have been a direct way to measure whether the OM9.2 T cells were specific for the ERV-K-Env epitope, discussions with commercial vendors determined that a 12–15 amino acid peptide was too long to synthesize as an HLA I-restricted dextramer.

Therefore, to address the perceived low affinity of the TCR with the peptide-MHC complex, we then added antigen presenting cells (APCs) to the ELISpot assays. Although free peptide is capable of binding to MHC molecules on T cells which can serve as weak antigen presenters to each other in an ELISpot assay, T cells biologically recognize an antigen best when it is presented by an antigen presenting cell [49]. To determine whether OM9.2 expressing cells could respond to the ERV-K-Env peptide when presented by a professional APC, we used the HLA-A*03:01 + Burkitt's lymphoma B cell line Raji, which is latently infected with Epstein-Barr virus (EBV) [50, 51]. Raji cells were pulsed with peptides prior to plating the ELISpot assay, to allow for uptake and presentation of the peptide, as has been previously described [45, 46] (Figure S3a). A higher level of IFN-γ secretion was observed from both OM9.2 T cells and untransduced T cells in the presence of unpulsed Raji cells (Figure S3b-d, "Raji", Figure S4a-c). The source of this increased IFN-γ secretion may be due to the HLA mismatching on the non-HLA-A*03:01 alleles between the T cells and the Raji cells, to T cell response to the EBV-infected Raji cells, or both [52–54]. However, compared to unpulsed Raji cells, OM9.2 T cells did not secrete more IFN-γ than untransduced T cells when cultured with any peptide-pulsed Raji cells at a low (200 ng) or high (10 μg) concentration of peptide (Figure S3b-d, "'antigen'-pulsed Raji"). These data demonstrate that the OM9.2 TCR did not respond to low or high concentrations of the ERV-K-Env peptide when presented by peptide-pulsed HLA-A*03:01 + Raji cells.

We then evaluated whether transduced T cells could respond to the ERV-K-Env peptide when it was presented by artificially generated APCs derived from the T cell donors, for a fully HLA-matched setting. We pulsed PBMCs from the same donors that the T cells were generated from with PHA to induce the formation of PHA-activated T cells (PHA blasts) (Figure S3e), which express high levels of HLA I [55]. Despite the complete HLA-matching of T cells to APCs, OM9.2 T cells still had low background secretion of IFN-γ when cultured with unpulsed PHA blasts or any peptide-pulsed PHA blasts compared to untransduced T cells (Figure S3f-g, Figure S4d-e) even in the presence of a high concentration of antigen. These data indicate that OM9.2 T cells did not respond to a high concentration of the ERV-K-Env peptide even when presented by HLA-matched artificially generated APCs.

Next, we used the most potent, professional APCs, dendritic cells (DCs), rather than artificially generated APCs. We matured monocyte-derived DCs from PBMCs from the same donor, as previously published [56], and repeated the experiment from Figure S3e-g, but with DCs instead of PHA blasts (Figure S3h). Again, we observed low secretion of IFN-γ when the OM9.2-expressing T cells were cultured with unpulsed DCs or any peptide-pulsed DCs compared to untransduced T cells (Figure S3i-j, Figure S4f-g). The high background level of IFN-γ is likely due to IFN-γ produced by DCs in response to the lipopolysaccharide added during the maturation protocol [57] (Figure S4f-g). Together, these data indicate that OM9.2-expressing T cells were not capable of specifically recognizing the ERV-K-Env epitope when presented by HLA-matched artificially generated APCs or professional APCs.

OM9.2 T cells were activated by a high concentration of the ERV-K-Env epitope when presented by HLA-A*03:01 + B LCLs

As a final test to determine whether the OM9.2 T cells could respond to the ERV-K-Env peptide, we used professional APCs derived from the original HIV-1 + HLA-A*03:01 + donor that the TCR was isolated from (donor OM9). There was also a high background level of IFN-γ secretion by OM9.2 T cells and untransduced T cells in response to the OM9 B LCLs (Fig. 3a-c, Figure S5, $n = 2$ donors, Figure S4h-j). Similar to the results observed with the Raji cells (Figure S3b-d), it cannot be determined whether this higher background level is due to the HLA mismatching on the non-HLA-A*03:01 alleles between the T cells and the OM9 B LCLs, to T cell response to the EBV-infected B LCLs, or both. Despite the elevated background signal to the OM9 B LCLs, OM9.2 T cells did not secrete significantly more IFN-γ than untransduced T cells when cultured with unpulsed B LCLs or OM9 B LCLs pulsed with 200 ng of peptide (Fig. 3a, Figure S5). However, in the presence of a high concentration of ERV-K-Env peptide, there was significantly more IFN-γ secreted by OM9.2 T cells in response to ERV-K-Env-pulsed OM9 B LCLs compared to untransduced T cells (Fig. 3b-c, $p = 0.0008$). We also observed a significant increase in the amount of IFN-γ secreted by OM9.2 T cells in response to ERV-K-Env-pulsed OM9 B LCLs compared to actin-pulsed OM9 B LCLs (Fig. 3c, $p = 0.0066$). Although we observed a significant increase in the amount of IFN-γ secreted by OM9.2 T cells in media alone, in response to unpulsed OM9 B LCLs, and actin-pulsed OM9 B LCLs compared to untransduced cells, these increases are smaller than the increase observed for the ERV-K-Env peptide and likely have minimal biological significance (Fig. 3c, $p = 0.015$, $p = 0.046$, $p = 0.0087$, respectively). As the OM9.2-expressing T cells only responded functionally to the ERV-K-Env peptide when it was present at a high concentration, these results support the findings from the paper where this ERV-K-Env-specific TCR was originally identified which

used high concentrations of peptide in IFN-γ ELISpot assays [38].

We then wanted to determine whether the ability of the OM9.2 T cells to respond to the ERV-K-Env peptide when presented by OM9 B LCLs extended to B LCLs from generated from another HLA-A*03:01 donor. This donor was HIV-1 seronegative, unlike donor OM9. We repeated the ELISpot assay with a high concentration of ERV-K-Env peptide and again observed a significant increase in IFN-γ secreted by OM9.2 T cells in response to ERV-K-Env-pulsed non-OM9 B LCLs compared to untransduced cells (Fig. 3d-f, $p = 0.004$, $n = 2$ donors, Figure S4k-l).

We also confirmed our IFN-γ ELISpot assay findings with intracellular cytokine staining for IFN-γ and another pro-inflammatory cytokine, TNF-α, via flow cytometry. Within the unsorted transduced T cells, we observed GFP + T cells produced significantly more TNF-α than GFP- T cells in the presence of peptide-pulsed non-OM9 B LCLs at all E:T ratios tested (Fig. 3g-h, n = 3 donors, $p = 0.0495$ for 1:1 and 10:1 E:T ratios in Fig. 3h; $p = 0.0463$ for 5:1 E:T ratio; p-values for all comparisons for intracellular cytokine staining are in Table S4). Interestingly, there was a slight reverse dose-dependence in which we observed less TNF-α as the E:T ratio increased. This trend was absent for cells producing IFN-γ alone but was present at the lower E:T ratios for cells producing both IFN-γ and TNF-α (Figure S8a-b, $p = 0.0495$ for 1:1 and 5:1 E:T ratios in Figure S8b). We also observed elevated production of TNF-α, but not IFN-γ alone or both IFN-γ and TNF-α, when looking at bulk CD3 + T cells instead of further gating on GFP + or GFP- cells (Figures S7-S8, $p = 0.0495$ for 1:1 and 5:1 E:T ratios in Figure S7b). Cumulatively, these data indicate that OM9.2 T cells can specifically respond to a high concentration of the ERV-K-Env peptide when it is presented by peptide-pulsed HLA-A*03:01 + B LCLs.

The ERV-K-Env epitope was not immunogenic in 3 healthy donors via in vitro priming

As the OM9.2 TCR appeared to have low affinity for the cognate peptide-MHC complex, we performed in vitro priming of peripheral blood mononuclear cells (PBMCs) with the ERV-K-Env 12mer/15mer to determine whether this epitope is naturally immunogenic. The in vitro priming workflow is outlined in Fig. 4a. Briefly, we used magnetic selection to separate PBMCs from healthy donors into CD14 + and CD14- fractions. The CD14 + cells were cultured in the presence of GM-CSF and IL-4 to promote development into DCs. Then DCs were loaded with various amounts of peptide and matured with a cocktail of activation cytokines. The peptide-loaded DCs were then used to stimulate the cryopreserved CD14- fraction along with T cell activation cytokines. Additional CD14 isolations were performed to stimulate the ongoing T cell cultures for a total of 2—3 stimulations. Cells were harvested a week after the final stimulation for functional assays.

To confirm that we could expand antigen-specific T cells using this protocol, we first expanded cells from 2 healthy donors against an overlapping peptide library

(See figure on next page.)

Fig. 3 OM9.2 T cells were activated by the ERV-K-Env peptide when presented by HLA-A*03:01 + B LCLs. **a**., **d**. Diagram of the ELISpot assay designs used in **b**.-**c**. and **e**.-**f**., respectively**,** Representative images of developed wells for OM9.2 T cell levels of background IFN-γ secretion (media) and IFN-γ secretion co-cultured with unpulsed and peptide-pulsed OM9-derived or non OM9-derived B LCLs for the ELISpot assays quantified in **c.** and **f**. Spot numbers are indicated to the bottom right of each image. Images shown for OM9.2 T cells. **c**., **f**. Number of IFN-γ spots per well normalized to the positive control (expressed as % of PHA) of untransduced T cells (black) and OM9.2 T cells (red) for the indicated conditions: Media = background level of IFN-γ secretion from T cells, B LCLs = background level of IFN-γ secretion from T cells co-cultured with unpulsed B LCLs, actin-pulsed B LCLs = negative control-pulsed B LCLs, ERV-K-Env-pulsed B LCLs = ERV-K-Env epitope-pulsed B LCLs, pp65-pulsed B LCLs = HLA-B*35 off-target control pulsed B LCLs, PHA = positive control. Each donor is indicated by a different symbol. ELISpot conditions were plated with the indicated peptide concentrations in duplicate or triplicate as cell numbers allowed for $n = 2$ donors (**c**) or $n = 3$ donors (**f**). **g**. Representative flow plots of intracellular IFN-γ and TNF-α staining from transduced T cells (gated on GFP + or GFP- cells) from Donor 272768 for the indicated conditions: T cells alone = background level of cytokine production from T cells, T cells + peptide = level of cytokine production from T cells in the presence of 50 µg peptide; various E:T ratios = level of cytokine production from T cells in the presence of decreasing numbers of unpulsed or peptide-pulsed non-OM9 B LCLs. B LCLs were pulsed with 10 µg peptide per million cells for 1 – 2 hours prior to plating with T cells. B LCLs and T cells were co-cultured for 6 hours in the presence of 1X protein transport inhibitors (cells alone, cells + peptide, or E:T conditions) or 1X stimulation cocktail (PMA/ionomycin). Flow gating strategy is in Figure S6c. h. Quantification of transduced T cells (GFP- = open red symbols/bars, GFP + = closed red symbols/bars) that stained positively for TNF-α alone for the indicated conditions. Each donor is indicated by a different symbol. Error bars represent SEM of all data points for all donors. The Wilcoxon rank sum test was used to compare values between untransduced and transduced T cells (indicated by *). The Kruskal Wallis test was used to compare the number of IFN-γ spots between each antigen condition for untransduced or transduced cells. Any Kruskal Wallis test that had $p < 0.05$ was followed by post-hoc pairwise Wilcoxon rank sum tests and adjusted for multiple comparisons (indicated by #). All statistical comparisons for ELISpot data are in Tables S1 and S2 and for intracellular cytokine staining in Table S4. *$p < 0.05$, **$p < 0.005$, ***$p < 0.0005$. ELISpot = Enzyme-linked immunosorbent spot; B LCL = B lymphoblastoid cell line; PMA = phorbol 12-myristate 13-acetate; SEM = standard error of the mean

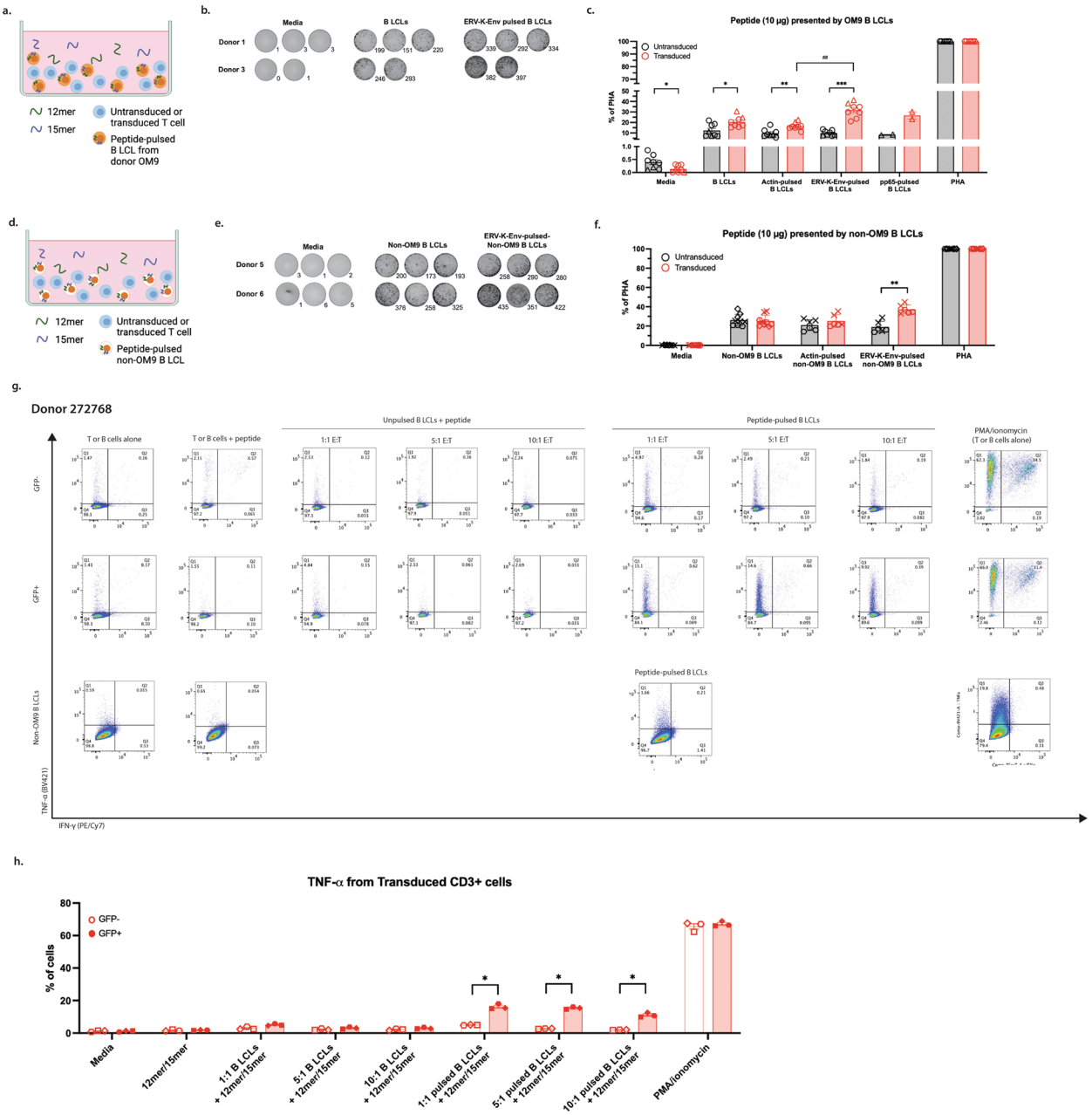

Fig. 3 (See legend on previous page.)

spanning the known tumor antigen PRAME [58]. T cells from both donors expanded over the course of the in vitro priming protocol, suggesting T cell activation occurred [59] (Figure S9a). IFN-γ ELISpot assays confirmed T cells expanded from both donors recognized PRAME (Figure S9b). Having confirmed we could expand antigen-specific T cells from healthy donors using this in vitro priming protocol, we then attempted to expand T cells from healthy donors against the ERV-K-Env 12mer/15mer. We loaded DCs with a low (100 ng, $n=3$ donors) or high (500 ng, $n=2$ donors) concentration of peptide. T cell fold-expansion was more donor-dependent than peptide concentration dependent (Fig. 4b). None of the T cells from any round of stimulation from any of the 3 donors demonstrated specificity for the ERV-K-Env epitope, as measured by IFN-γ ELISpot assays (Fig. 4c-d, p-values from all statistical comparisons for ELISpot data are in Tables S5 and S6). There was slightly higher background IFN-γ secretion from T cells cryopreserved after stimulations 1 and 2, likely due to the freeze/thawing procedure

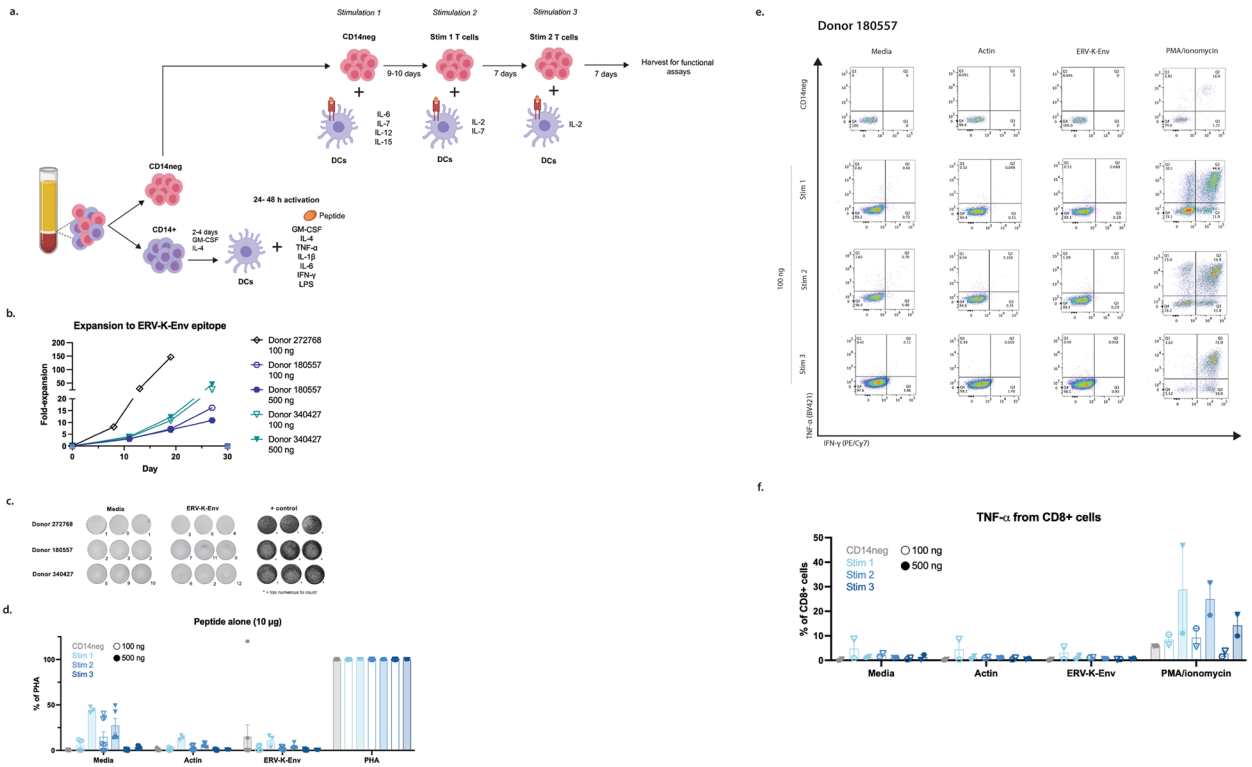

Fig. 4 In vitro priming of cells with the ERV-K-Env epitope did not result in antigen-specificity. **a**. Magnetic selection is used to separate PBMCs from healthy donors into CD14 + and CD14- fractions. The CD14 + cells were cultured in the presence of GM-CSF and IL-4 to promote development into DCs. Then DCs were loaded with various amounts of peptide and matured with a cocktail of activation cytokines. The peptide-loaded DCs were then used to stimulate the cryopreserved CD14- fraction along with T cell activation cytokines. Additional CD14 isolations were performed to stimulate the ongoing T cell cultures for a total of 2—3 stimulations. Cells were harvested a week after the final stimulation for functional assays. **b**. Fold-expansion of T cell lines from each donor over the course of the expansion towards the indicated amounts of the ERV-K-Env epitope. **c**. Representative images of developed wells of T cells from each donor expanded against the ERV-K-Env peptide. Images shown are for T cells from stimulation 3, 100 ng of peptide for background IFN-γ secretion (media), IFN-γ secretion in the presence of 50 µg of ERV-K-Env peptide, and IFN-γ secretion in the presence of the positive control. Number of spots in each well are indicated to the bottom right of each image**.** Number of IFN-γ spots per well normalized to the positive control (expressed as % of PHA) of T cells from each round of stimulation (increasing shades of blue) for the indicated conditions: Media = background level of IFN-γ secretion from T cells, actin = negative control, ERV-K-Env = ERV-K-Env 12mer/15mer, + PHA = positive control. Each donor is indicated by a different symbol. Open symbols indicate T cells expanded against 100 ng of peptide. Closed symbols indicate CD14- cells or T cells expanded against 500 ng of peptide. Error bars represent SEM of all data points for all donors. ELISpot conditions were plated in duplicate or triplicate as cell numbers allowed. The Kruskal Wallis test was used to compare the number of IFN-γ spots between T cells in the presence of each antigen. Any Kruskal Wallis test that had $p < 0.05$ was followed by post-hoc pairwise Wilcoxon rank sum tests and adjusted for multiple comparisons using the Bonferroni correction. *$p < 0.05$, **$p < 0.005$, ***$p < 0.0005$. **e**. Representative flow plots for intracellular IFN-γ and TNF-α of cells from each round of stimulation from Donor 180557 in the presence of media (background), actin (negative control), ERV-K-Env epitope, or PMA/ionomycin (positive control). Cells were cultured for 6 hours in the presence of 1X protein transport inhibitors (media, actin, ERV-K-Env epitope) or 1X stimulation cocktail (PMA/ionomycin). Flow gating strategy is in Figure S10. $N = 1$ technical replicate for each donor. **f**. Quantification of CD8 + T cells from 3 healthy donors that stained positively for TNF-α. Increasing shades of blue indicate T cells from each round of peptide stimulation. Each donor is indicated by a different symbol. Open symbols indicate T cells expanded against 100 ng of peptide. Closed symbols indicate CD14- cells or T cells expanded against 500 ng of peptide. Error bars represent SEM of all data points for all donors. DC: dendritic cell; GM-CSF: granulocyte–macrophage colony stimulating factor; LPS: lipopolysaccharide; ELISpot = Enzyme-linked immunosorbent spot; PHA = phytohemagglutinin; SEM = standard error of the mean

(Fig. 4d, "Media"). Interestingly, this higher background IFN-γ secretion was not observed in the actin or ERV-K-Env conditions. Importantly, all T cells demonstrated functional capability as they secreted IFN-γ in the presence of PHA.

We again confirmed our IFN-γ ELISpot assay findings with intracellular cytokine staining for IFN-γ and TNF-α. In agreement with the ELISpot data, we did not observe significant increases in staining for IFN-γ or TNF-α in CD4 + or CD8 + T cells at any round of stimulation from any of the 3 donors (Fig. 4e-f, Figure S11). The flow gating

strategy for this intracellular cytokine staining is depicted in Figure S10. Again, we observed that all cells could produce both IFN-γ and TNF-α as there was positive staining for both markers in T cells in the presence of a stimulation cocktail containing PMA/ionomycin.

We reasoned that while the ERV-K-Env epitope was not immunogenic in any of the 3 healthy donors we tested via in vitro priming, another portion of the ERV-K TE might be. We then attempted to expand T cells from one of the same healthy donors used in both the PRAME and ERV-K-Env in vitro priming experiments (Donor 272768) against an overlapping peptide library spanning the *gag* gene of ERV-K 6 (Uniprot Q7LDI9). Despite having a decent fold-expansion (190-fold), T cells expanded against 100 ng of the ERV-K-Gag overlapping peptide library did not recognize the antigen in IFN-γ ELISpot assays (Figure S9c-d, "100 ng, rep 1").

We then wanted to determine whether altering the amount of peptide used to load into DCs during the activation step could help with T cell expansion towards ERV-K-Gag, as the peptide concentration used in this step has been shown to alter the size of the activated T cell population [60]. To do this, we repeated this expansion with cells from Donor 272768, but altered the amount of peptide to be 100-fold lower, the same as the previous expansion, or tenfold higher during the DC peptide-loading step (Figure S9c-d, "1 ng", "100 ng, rep 2", and "1 μg", respectively). While all 3 of these T cell lines had very high fold-expansion (314-fold for 1 ng, 623-fold for the same concentration, and 352-fold for 1 μg), none of the T cell lines demonstrated specificity for ERV-K-Gag, as measured by IFN-γ ELISpot assay (Figure S9c-d).

At this point, we hypothesized that the precursor frequency of ERV-K-specific T cells was extremely low in peripheral blood and that enriching the starting CD14- population for memory T cells would increase this precursor frequency by depleting naïve T cells [61–63]. We performed a new round of in vitro *priming* against the overlapping library of ERV-K-Gag using either bulk CD14- T cells, CD45RO-negative cells (enriched for naïve CD45RA + cells), or CD45RO + cells (enriched for memory CD45RO + cells) from a new donor (Donor 180557). The fold-expansion of the products dipped after the second stimulation but increased after the third stimulation. Interestingly, the CD45RO-negative cells (enriched for naïve cells) expanded the most (21-fold) compared to the bulk CD14- (12-fold) and CD45RO + cells (13-fold), which was the opposite of what we hypothesized (Figure S9e). However, none of the expanded T cell populations from this new donor were specific for ERV-K-Gag, as measured by IFN-γ ELISpot (Figure S9f).

Finally, we tried expanding T cells isolated from cells from patients with OC against ERV-K-Gag, as it has been reported that ERV-K-Env-specific T cells could not be expanded from healthy donors, but could be expanded from PBMCs isolated from a patient with OC [29]. We obtained drained ascites fluid from a patient with OC (Patient KBC-002) and separated the tumor infiltrating lymphocytes (TILs) from the tumor cells. We also obtained PBMCs from this patient as well and carried out the in vitro priming protocol using either the TILs or the PBMCs are starting material. We also expanded T cells from another patient with cancer, Patient KBC-007. The fold-expansions for these T cells were not as good as those from healthy donors (Figure S9g-h, for Patient KBC-002: ascites- blue star, PBMCs- blue circle). Although the final T cell product derived from the TILs expanded more than the product derived from the PBMCs (24-fold expansion for the product derived from TILs compared to 0-fold expansion for the product derived from PBMCs), this is likely an artifact of the repeated freeze-thawing of the T cells that occurred throughout the expansion protocol for the product derived from the PBMCs (Figure S9g). Neither T cell product expanded from the TILs from Patient KBC-002 or PBMCs from Patient KBC-007 were specific for the overlapping ERV-K-Gag peptide library as measured by IFN-γ ELISpot (Figure S9h). Together, these data suggest that T cells specific for the ERV-K-Env 12mer/15mer epitope or an overlapping peptide library of ERV-K-Gag cannot be expanded from healthy donors using this in vitro priming method. Additionally, T cells specific for ERV-K-Gag were unable to be expanded from cells isolated from 2 patients with cancer.

Discussion

The ability of the OM9.2 TCR to recognize and kill HIV-1-infected cells, coupled with the defined expression of ERVs in various cancers, including OC, suggests that this TCR may be repurposed to treat patients with HLA-matched solid tumors. However, we found that the ability of the ERV-K-Env TCR to recognize and kill HIV-1-infected cells does not translate well to the setting of healthy donors, suggesting that the OM9.2 TCR is a poor candidate for T cell targeting of this epitope. Additionally, we demonstrated via in vitro priming that the ERV-K-Env epitope does not elicit an immune response in T cells expanded from healthy donors.

Here, we first demonstrated that T cells derived from healthy donors transduced with the OM9.2 TCR were only capable of being activated by the cognate peptide when it was a) present at high concentrations and b) presented by peptide-pulsed HLA-A*03:01 B LCLs. These results agree with the study in which this T cell clone was originally identified [38]. In that study, the ERV-K-Env-specific CD8 + T cell clone derived from donor OM9

secreted IFN-γ in response to high concentrations (tens of micrograms amounts) of the ERV-K-Env epitope in the presence of B LCLs derived from donor OM9, as we observed in our study. In contrast, tumor-specific T cells are typically able to secrete IFN-γ in response to their cognate peptides at concentrations as low as a few hundred nanograms without professional APCs present [59, 64]. The high concentration of peptide required to elicit a T cell response suggests that the OM9.2 TCR is of low affinity for the cognate peptide-MHC complex.

While the results in our study confirm those of Jones et al., they conflict with the findings from Rycaj et al., in which T cells expanded from patients with OC were able to secrete IFN-γ in response to ERV-K-Env [29]. A few key differences between our study and the Rycaj et al. study may account for the disparate findings. One major difference is that Rycaj et al. used the entire ERV-K-Env protein as the antigen, rather than the minimal 12mer/15mer epitope used in our study. It is likely that the epitope (or epitopes) eliciting an IFN-γ response from the T cells in the Rycaj et al. study is not the epitope targeted by the OM9.2 TCR. Another difference from the Rycaj et al. study is that T cells were expanded against ERV-K-Env from patients with OC while our study used mostly T cells isolated from healthy donors. Although T cells transduced with the ERV-K-Env TCR should recognize the epitope regardless of the donor, this difference further suggests that the ERV-K-Env epitope targeted by the OM9.2 TCR is not contributing to the IFN-γ response seen in the Rycaj et al. study. Another publication from the same group demonstrated IFN-γ secretion against ERV-K from T cells expanded from patients with breast cancer, but not T cells expanded from healthy donors [65]. When combined with our data, these findings suggest that even though the HLA-A*03:01-restricted epitope was poorly targeted by the OM9.2 TCR, another TCR targeting this epitope or the targeting of other portions of the ERV-K-Env surface domain may yield better T cell responses.

As the only professional APC capable of eliciting a T cell response to the ERV-K-Env peptide is B LCLs, this suggests that latent infection of professional APCs may somehow be facilitating alternative processing and presentation of this epitope. While we initially concluded that the seropositivity of the OM9 donor for HIV-1 + could be contributing to the ability of the OM9 B LCLs to present the antigen in a way that is recognized by this TCR, the data with the non-OM9 B LCLs suggest that HIV-1 seropositivity does not contribute to the B LCLs' ability to present this antigen to T cells. Instead, the latent infection of B LCLs with EBV might be contributing to the ability of these APCs to present the ERV-K-Env peptide efficiently. It is worth noting that although we saw no response from OM9.2 T cells to the peptide presented by Raji cells, these cells are also latently infected with EBV [52, 53]. However, the malignant state of Raji cells may contribute to their inability to present this peptide. Still, the possibility of only latently infected cells being able to present this unusually long HLA-A*03:01-restricted peptide cannot be ruled out by the experiments in this work alone.

Some elements of our study design limit the conclusions we can draw from our data. First, we used the level of GFP expression as a surrogate marker of the ERV-K-Env TCR expression. While the use of a tetramer would have directly confirmed surface expression of the TCR, discussions with commercial vendors concluded that generating an MHC I tetramer with a 12- or 15-amino acid peptide in the peptide-binding groove would not be feasible. However, the observation of OM9.2 T cell specificity for the ERV-K-Env epitope in this work suggest that the TCR was expressed on the surface of the transduced T cells. Second, we were limited in the number of donors that we used in our study. Individual experiments for the TCR included 6 donors and in vitro priming experiments for the ERV-K-Env epitope included 3 donors. Third, the high background level of IFN-γ secretion by the T cells in the presence of some APCs—in particular Raji cells, DCs, and B LCLs—made it difficult to determine if the T cells recognized the ERV-K-Env peptide. However, the high concentration of the ERV-K-Env peptide used in Fig. 3 resulted in sufficient activation of OM9.2 T cells to be observed even in the presence of this high background signal. The data from these experiments and the controls (Figure S4) suggest that the signal seen in Fig. 3 is not just background IFN-γ secretion upon recognition of APCs.

As the OM9.2 TCR appeared to have low affinity for the targeted ERV-K-Env epitope, we also investigated whether the epitope could elicit an immune response in healthy donors via in vitro priming. While we could expand PRAME-specific T cells from healthy donors using an established in vitro T cell expansion protocol, we were unable to expand T cells specific for the ERV-K-Env epitope using the same protocol. We also were unable to expand ERV-K-Gag-specific T cells from healthy donors or patients with cancer. The size of this overlapping peptide library ($n = 172$ peptides) is not a concern for DC uptake as antigen-specific T cells have been expanded using this protocol with peptide libraries consisting of more than 300 individual peptides [66].

We then reasoned that while the number of peptides was not an issue, the concentration of peptides added to the DCs could affect the stimulation of an antigen-specific T cells. A study by Bullock and colleagues showed that the concentration of peptide used to pulse DCs affects the magnitude of the antigen-specific T

cell populations [60]. This study showed that although expression of stable surface HLA molecules increases with increasing peptide concentration, antigen-specific CD8 + T cells showed increasing levels of activation in the presence of the peptide at concentrations of 0.1 μg/mL to 1 μg/mL, then decreased at higher peptide concentrations. The peptide concentrations we use in our in vitro priming protocol are normally 0.1 μg/mL, which is on the lower end of what Bullock et al. reported. Therefore, we attempted a new round of T cell expansions in which we pulsed DCs with peptide concentrations 100-fold lower (1 ng/mL) and tenfold higher (1 μg/mL). Interestingly, the T cells activated with DCs pulsed with each of the modified peptide concentrations expanded less than T cells activated with DCs pulsed with the previously used peptide concentration of 0.1 μg/mL. These data suggest that the 0.1 μg/mL peptide concentration may be the optimal concentration to expand T cells using this protocol. However, none of the T cells activated with DCs pulsed with any of the three concentrations of ERV-K-Gag demonstrated specificity for this antigen.

One aspect of the in vitro priming protocol that we did not investigate in our optimizations but is known to affect the observed frequency of antigen-specific T cells is the number of DCs used to stimulate the T cells. A study by Wölfl and Greenberg tested several ratios of DCs:T cells to expand human CD8 + T cells specific for an HLA-A*02:01-restricted epitope within the human Melan-A (or MART1) protein [67]. Their data showed that the frequency of human CD8 + T cells specific for this antigen increases as the ratio of DCs:T cells increases, with the highest frequency of antigen-specific T cells observed using a ratio of 1:4 DCs:T cells and the lowest frequency at a ratio of 1:128 DCs:T cells. While we used a similarly high ratio of DCs:T cells in our expansion protocol (1:10 DCs:T cells), we could have further increased this ratio to expand an observable antigen-specific population against ERV-K-Gag.

We then hypothesized that perhaps ERV-K-Env- or ERV-K-Gag-specific T cells could only be expanded from the memory compartment of T cells where tumor-specific T cells have been shown to reside [61–63]. The viability of all T cell products generated in this round of expansions decreased overtime, which may be due to the fact that these expansions were done in T-25 and T-75 flasks to maximize the ratio of DCs to T cell precursor frequency. As the in vitro priming protocol is usually done in 24-well plates, the density of the cells in the flasks might have been too low for the T cells to expand as efficiently as they do when they are more crowded in plates. Despite these low viabilities, the T cells did expand, but were not specific for the ERV-K-Gag overlapping peptide library as measured by IFN-γ ELISpot or intracellular cytokine staining.

As we appeared to have exhausted experimental manipulations to expand TE-specific T cells from healthy donors, we moved to using cells isolated from cancer patients. Our rationale for this switch was due to the previously discussed report from Rycaj and colleagues that demonstrated ERV-K-Env-specific T cells could only be expanded from a patient with OC and not several healthy donors [29]. Although the T cells expanded from the TILs of Patient KBC-002 against ERV-K-Gag were not specific for this antigen, they had decent fold-expansion. However, cell numbers were insufficient in the T cells expanded from the PBMCs of this patient due to multiple freeze-thaws of the T cells during the in vitro priming protocol, which prevented further head-to-head comparison of these products. We also did not observe specificity for the ERV-K-Gag antigen by T cells expanded from the PBMCs of a second donor with OC.

Collectively, this study provides evidence that the OM9.2 TCR is a poor candidate for T cell targeting of this epitope due to a) no increased response from OM9.2 T cells in the presence of HLA-A*03:01 OC cells compared to untransduced T cells and b) an increased response from OM9.2 T cells only in the presence of high concentrations of the ERV-K-Env peptide when presented by peptide-pulsed HLA-A*03:01 B LCLs. Additionally, we showed that this epitope did not elicit an immune response in healthy donors via in vitro priming. We also demonstrated that expanding cells from healthy donors or cells isolated from patients with OC were not specific for an overlapping peptide library of another gene of ERV-K, *gag*. These results conflict with recent reports that identified immunogenic epitopes from ERV-K-Gag and ERV-K-Pol in cancer settings [68, 69]. In these studies, T cells expanded via in vitro priming against these ERV-K-derive epitopes were able to recognize and kill cancer cells. However, these epitopes were HLA-A*02:01-restricted and not HLA-A*03:01-restricted, as was the epitope investigated in this study.

Despite our lack of success in the described experiments, many recent reports have shown that TE-derived antigens are presented by MHC on tumor cells [70–73]. While these studies confirm the existence of TE-derived antigens presented by tumor cells, it remains to be determined whether T cells can be reliably generated to recognize and respond to these antigens alone. A recent report showed that a T cell receptor that recognizing an HLA-A*11-restricted epitope of ERV-E mediated regression of clear cell renal carcinoma in a murine xenograft model [74]. Moreover, these preclinical findings provided the basis for the first clinical trial evaluating TCR-engineered T cells targeting an ERV in clear cell renal cell carcinoma,

which induced tumor regression in one patient with metastatic disease (NCT03354390) [75]. Beyond targeting whole TEs as tumor associated antigens, a more effective approach may be to target chimeric TE-derived transcripts, which derive from cryptic promoters within TEs [70]. A pan-cancer analysis of over 30 tumor types in The Cancer Genome Atlas have shown these TE-derived chimeric transcripts to be immunogenic antigens. These TE-derived antigens may boost immune recognition of tumors, thus resulting in increased control of disease over time and ultimately, longer survival for patients with malignancies, both with OC and beyond.

Conclusions

This study demonstrates that the OM9.2 TCR is not a good candidate for targeting the ERV-K-Env epitope investigated here. The cognate epitope was only recognized at high concentrations when presented by peptide-pulsed HLA-A*03:01 B LCLs. In vitro priming efforts of cells from healthy donors against the epitope also did not result in antigen specificity. Further in vitro priming experiments against an overlapping peptide library of ERV-K-Gag using cells from healthy donors or cells isolated from patients with cancer were also unsuccessful. Future efforts to develop TE-derived T cells for OC should focus on other TCRs for this epitope, other epitopes within ERV-K-Env, or other TE-derived targets, such as chimeric TE-derived peptides.

Methods

Aim

To determine the efficacy of the ERV-K-Env TCR to recognize its cognate epitope as a therapeutic option for OC.

Design

Use of in vitro experiments to transduce cells from primary healthy donors and measure T cell functionality as well as in vitro priming of PBMCs from healthy donors.

Setting: In vitro.

Plasmid preparation

The OM9.1 ERV-K-Env TCR plasmid construct was a kind gift from Dr. Mario Ostrowski. The OM9.1 construct was further optimized (construct OM9.2) by cloning it into a lentiviral vector under the control of the EF-1α promoter and confirmed by Sanger sequencing. For Donors 1–6, construct OM9.2 was transformed into Agilent XL1 Blue Supercompetent cells (Agilent, Cat. #200236), according to the manufacturer's instructions. Plasmid pMD2.G (Addgene, Cat. #12259) was transformed into 5-alpha competent E. coli cells (NEB, Cat. #C2987I), according to the manufacturer's instructions. Plasmids pRSV.Rev (Addgene, Cat. #12253) and pMDLg/RRE (Addgene, Cat. #12251) were obtained as agar stabs. For Donors A-C, the OM9 TCR and packaging plasmids (all from Dr. Mario Ostrowski) were transformed into 5-alpha competent E. coli cells (NEB, Cat. #C2987I) according to the manufacturer's instructions. Plasmids were isolated from bacterial pellets using the PureLink HiPure Plasmid Midiprep kit (Invitrogen, Cat. #K210004) according to the manufacturer's instructions.

Cell sources

We have received the following cell lines from Dr. Dennis Slamon's laboratory: ES-2 and TOV112D. Cell lines were tested using a short tandem repeat (STR) profiling service provided by the Johns Hopkins Genetic Resources Core Facility (GRCF). STR profiling by the GRCF is carried out following the ANSI/ATCC ASN-0002–2011, Authentication of Human Cell Lines: Standardization of STR Profiling. For cell lines derived from repositories, the profile of the cell line is used for comparison using verification tools found on the repository web sites to determine relatedness of the line to those held by the repositories. GRCF uses the following databases to generate the reports: Leibniz Institute DSMZ German Collection of Microorganisms and Cell Cultures, American Tissue Culture Collection, Japanese Collection of Research Bioresources. The algorithms used in the American National Standards Institute (ANSI) and the American Type Culture Collection Standards Development Organization's (ATCC SDO) report ANSI/ATCC ASN-0002–2011 are used to calculate percent match or evaluation value (EV) which were then reported to our lab. 293 T cells (Cat. #CRL-3216), SupT1 cells (Cat. #CRL-1942), and Raji cells (Cat. #CCL-86) were purchased from ATCC. B LCLs were kind gifts from Dr. R. Brad Jones (OM9 B LCLs) and Dr. Catherine M. Bollard (non-OM9 B LCLs). In general, B lymphoblastoid cells (B LCLs) were generated by immortalizing B cells from donor OM9 with the B95-8 Epstein-Barr virus according to published protocols [76]. De-identified healthy donor peripheral T cells were purchased from the Human Immunology Core at the University of Pennsylvania, de-identified commercially available buffy coats were purchased from New York Blood Center (New York, NY), and de-identified platelet filters were purchased from Oklahoma Blood Institute (Oklahoma City, NY). PBMCs and ascites samples were obtained with informed consent from patients at the GW University Hospital in Washington, DC in accordance with Institutional Review Board protocol #180205. Cells were tested for mycoplasma yearly using the MycoAlert® Kit (Lonzo, Cat #LT07-703).

Table 1 Surface antibodies used in flow cytometry experiment. Vendor, catalogue, and titration information for surface antibodies used in flow cytometry experiments (Figure S2c)

Marker	Cellular location	Fluorophore	Supplier	Catalogue #	µL antibody per million cells
CD3	Surface	BV605	Biolegend	317322	1
TCR-α/β	Surface	APC	Biolegend	306718	1

Peptides

The ERV-K-Env 12mer/15mer was custom synthesized by the proteomics core at Children's National Hospital (Washington, DC). Actin and PRAME overlapping peptide libraries were purchased from JPT (PM-ACTS and PM-OIP4, respectively). The ERV-K-Gag overlapping peptide library was custom synthesized by GenScript (Piscatway, NJ).

Lentiviral transduction of T cells

Lentivirus production 293 T cells were cultured in DMEM (Corning, Cat. #10–013-CV) + 10% FBS (R&D Systems, Cat. #S12450H) + 1% penicillin/streptomycin (Gibco, Cat. #15070063). On the day of transfection, the media was replaced with T cell media (RPMI [Corning, Cat. #10–040-CV] + 10% FBS + 1% penicillin/streptomycin + 1X MEM non-essential amino acids (MEM NEAA) [Corning, Cat. #25–025-CI] + 1X GlutaMAX [Gibco, Cat. #35050–061] + 10 mM HEPES [Gibco, 15630–080]). Lentivirus was made by combining the appropriate plasmids with OptiMEM (Gibco, Cat. #11058–021), adding the plasmid mixture to 293 T cells, and harvesting at 48 h by filtering through a 0.45 µm PVDF filter (CellTreat, Cat. #229745).

Activation and lentiviral transduction of T cells Isolated T cells were activated with anti-CD3/anti-CD28 Dynabeads (Gibco, Cat. #11131D) and 30 U/mL recombinant human IL-2 (Peprotech, Cat. #200–02). T cells were plated and rested overnight at 37 °C prior to transduction. T cells were transduced with lentivirus (construct OM9.2 for SupT1 cells and Donors 1–6 and construct OM9.1 for Donors A-C) and transduction efficiency was measured by detection of eGFP-fluorescence using a BD LSR Fortessa, a BD FACS Celesta, or a BD Influx cytometer.

Interferon-γ ELISpot

Wells of a PVDF-membrane plate (Millipore Sigma, Cat. #MSIPS4W10) were activated with 70% ethanol then coated with 1 µg of anti-human-IFN-γ antibody 1-D1K (Mabtech, Cat. # 3420–3-1000, RRID #AB_907282). The plate was incubated at room temperature for at least 4 hours or overnight at 4°C. Antigens were plated at 200–400 ng per well for low concentration and 10 µg per well for high concentration. Phytohemagglutinin (PHA, Thermo Fisher Scientific, Cat. #R30852801) was plated at 1–5 µg per well. Cells were plated at 1×10^5 cells/well (co-culture conditions contained 1×10^5 cells of each type) in duplicate or triplicate as cell numbers allowed. The plate was incubated overnight at 37°C. Spots were developed with 0.1 µg of biotinylated anti-IFN-γ 7-B6-1 antibody (Mabtech, Cat. #3420–6-1000, RRID #AB_907273), followed by the Vectastain Elite ABC-HRP Kit (Vector Laboratories, Cat. #PK-6100), and 3-amino-9-ethylcarbazole (Sigma Aldrich, Cat. #A6926). Wells were imaged and counted using an AID vSpot Spectrum plate reader (Autoimmun Diagnostika GMBH).

Flow cytometry and intracellular cytokine staining

To assess the optimization of the OM9.2 construct, cells were stained with Live/dead Fixable Aqua (Invitrogen, Cat. #L34965) and the antibodies diluted to titrated amounts indicated in Table 1 in Facs buffer (PBS + 1% FBS). For intracellular cytokine staining of OM9.2-expressing T cells, non-OM9 B LCLs were pulsed with 10 µg peptide per million cells for 1–2 hours at 37 °C. B LCLs and T cells were plated alone or in co-culture at a ratio of 1:1, 5:1, or 10:1 in T cell media (RPMI + 10% FBS + 1% penicillin/streptomycin + 1X MEM NEAA + 1X GlutaMAX + 1 mM HEPES) and incubated at 37°C. At the time of plating, 1X protein transport inhibitors (Invitrogen, Cat. #00–4980-93) or 1X cell stimulation cocktail (Invitrogen, Cat. #00–4970-93) were added and cells were incubated at 37°C for 6 hours. For the in vitroprimed cells, the indicated cell types were plated in the presence of media, 50 ng/µL actin pepmix, or 50 ng/µL ERV-K-Env 12mer/15mer. At the time of plating, 1X protein transport inhibitors or 1X cell stimulation cocktail were added to cells, then incubated at 37°C for 6 hours. Cells were stained with the viability marker listed above, the surface antibodies diluted to titrated amounts indicated in Table 2, fixed in Cytofix/Cytoperm solution (BD, Cat. #51-2090KZ), and permeabilized with 1X permeabilization/wash buffer (BD, Cat. #51-2091KZ). Permeabilized cells were stained with appropriate diluted antibodies or 1X permeabilization buffer. Data was acquired using

Table 2 Surface antibodies used in intracellular cytokine staining. Vendor, catalogue, and titration information for surface and intracellular antibodies used in flow cytometry experiments (Figs. 3g-h, 4e-f and Figures S6c, S7, S8, S10, and S11)

Marker	Cellular location	Fluorophore	Supplier	Catalogue #	µL antibody per million cells
CD45	Surface	BV640	Biolegend	304044	2.5
CD3	Surface	PerCP/Cy5.5	Biolegend	300328	0.625
CD4	Surface	APC	Biolegend	357407	2.5
CD8	Surface	BV785	Biolegend	301046	1.25
CD19	Surface	APC/Cy7	Biolegend	363010	1.25
CD16	Surface	FITC	BD	560996	4
CD56	Surface	BV605	Biolegend	318334	2
HLA-A*03	Surface	PE	Invitrogen	12–5754-42	0.625
IFN-γ	Intracellular	APC	Biolegend	502512	5
IFN-γ	Intracellular	PE/Cy7	Biolegend	502527	5
TNF-α	Intracellular	BV421	Biolegend	502932	2.5

a BD FACS Celesta and analyzed using FlowJo v10.8.1 with manual compensation using single stained cells and UltraComp eBeads (Thermo Fisher Scientific, Cat. #01–2222-41).

In vitro priming experiments

T cell lines were generated from PBMCs using monocyte-derived DCs based on previously established protocols with minor modifications [77, 78], as illustrated in Fig. 4a. Briefly, monocytes were isolated from PBMCs using a CD14 isolation MACS MicroBeads kit (Miltenyi Biotec, Cat. #130–050-201) according to the manufacturer's instructions using 2 µL of beads and 3 µL MACS buffer (PBS, 0.5% bovine serum insulin [BSA] [Sigma Aldrich, Cat. # A9418], 2 mM EDTA [Thermo Fisher Scientific, Cat. #15575020]) per million cells. The isolated CD14 positive (CD14+) cells were cultured in DC media (CellGenix GMP DC media [CellGenix, Cat. #20801], 1% GlutaMAX [Gibco, Cat. #35050–061], 1% penicillin/streptomycin) in the presence of 800 U/mL granulocyte–macrophage colony-stimulating factor (GM-CSF) (R&D Systems, Cat. #215-GM) and 1,200 U/mL interleukin (IL-4) (R&D Systems, Cat. #204-IL). The CD14-negative (CD14neg) fraction was cryopreserved for later use. The CD14+cells (now termed DCs) were fed with GM-CSF and IL-4 on day 2 or 3. DCs were pulsed two days after feeding with 100 ng or 500 ng of peptide. After 4 – 6 hours of incubation at 37°C with peptide, DCs were activated for antigen presentation for 24 – 48 h at 37°C with 800 U/mL GM-CSF, 1,200 U/mL IL-4, 10 ng/mL tumor necrosis factor-α (TNF- α) (R&D Systems, Cat. #210-TA), 10 ng/mL IL-1β (R&D Systems, Cat. #201-LB), 100 ng/mL IL-6 (R&D Systems, Cat. #206-IL), 100 U/mL interferon-γ (IFN-γ) (R&D Systems, Cat. #285-IF), and 30 ng/mL lipopolysaccharide (LPS) (Sigma Aldrich, Cat. #L4391). DCs were harvested and pulsed with 100 ng or 500 ng peptide for 30 min at 37 °C. The cryopreserved CD14neg cells were thawed and stimulated with the harvested DCs at a 1:10 (DC:T cell) ratio in T cell media (47% RPMI, 47% Click's media [Irvine Scientific, Cat. #9195], 5% human AB serum [BIOIVT, Cat. #HUMANSRM], 1% GlutaMAX) supplemented with 100 ng/mL IL-6, 10 ng/mL IL-7 (R&D Systems, Cat. #207-IL), 10 ng/mL IL-12 (R&D Systems, Cat. #219-IL) and 5 ng/mL IL-15 (R&D Systems, Cat. #24-ILB). Extra matured and activated DCs were cryopreserved for subsequent stimulations. If CD45RO isolation was performed, the cryopreserved CD14- cells were thawed and put through a CD45RO isolation MACS MicroBeads kit (Miltenyi Biotec, Cat. # 130–046-001) according to the manufacturer's instructions. CD14- and CD45RO+cells were incubated at 37°C and were expanded with 100 ng/mL IL-6, 10 ng/mL IL-7, 10 ng/mL IL-12, and 5 ng/mL IL-15. CD45RO- cells were incubated at 37°C and were expanded with 60 ng/mL IL-21 (R&D Systems, Cat. #8879-IL-010). CD45RO- cells were fed 2 days after stimulation 1 with 100 ng/mL IL-6, 10 ng/mL IL-7, 10 ng/mL IL-12, and 5 ng/mL IL-15. All stimulation 1 T cells were fed and/or split as needed with 10 ng/mL IL-7 and 5 ng/mL IL-15 for a total of 9 – 10 days after stimulation 1. A new CD14 isolation were repeated for subsequent stimulations if needed, otherwise cryopreserved matured and activated DCs were thawed on the day of the next stimulations, pulsed with 100 ng or 500 ng peptide for 30 min at 37°C, then used to stimulate the ongoing T cell culture at a 1:10 ratio (DC:T cell) in the presence of 10 ng/mL IL-7 and 50 U/mL IL-2 (Peprotech, Cat.

#200–02). T cells were fed and split with fresh media and alternating between 5 ng/mL IL-15 or 50 U/mL IL-2, as needed for 7 days. If needed, a new CD14 isolation was performed for the third stimulation, otherwise cryopreserved matured and activated DCs were thawed on the day of the third stimulation, pulsed with 100 ng or 500 ng peptide for 30 min at 37°C, then used to stimulate the ongoing T cell culture at a 1:10 ratio (DC:T cell) in the presence of 50 U/mL IL-2. T cells were fed and split with fresh media and alternating between 5 ng/mL IL-15 or 50 U/mL IL-2, as needed for 7 days. T cell products were harvested for functional assays. Expansion was quantified by harvesting and counting with trypan blue or acridine orange staining on days of T cell stimulation and/or harvest.

Statistics

Statistics were performed in RStudio v4.0.1. The Wilcoxon rank sum test was used to compare the number of IFN-γ spots or percentage of intracellular cytokine staining between untransduced and transduced T cells (indicated by *). The Kruskal Wallis test was used to compare the number of IFN-γ spots between each antigen condition. Any Kruskal Wallis test that had $p < 0.05$ was followed by post-hoc pairwise Wilcoxon rank sum tests and adjusted for multiple comparisons using the Bonferroni correction (indicated by #). Values from all statistical comparisons are in Tables S1, S2, S4-S6. $^{*}p < 0.05$, $^{**}p < 0.005$, $^{***}p < 0.0005$.

Abbreviations

TE	Transposable element
OC	Ovarian cancer
ERV-K-Env	Endogenous retrovirus K *env*
HIV-1	Human immunodeficiency virus-1
PBMC	Peripheral blood mononuclear cell
HLA	Human leukocyte antigen
IFN-γ	Interferon-γ
APC	Antigen presenting cell
EBV	Epstein Barr Virus
DC	Dendritic cell
B LCL	B lymphoblastoid cell line

Supplementary Information

The online version contains supplementary material available at https://doi.org/10.1186/s13100-024-00333-w.

Supplementary Material 1.

Supplementary Material 2.

Supplementary Material 3.

Supplementary Material 4.

Supplementary Material 5.

Supplementary Material 6.

Supplementary Material 7.

Acknowledgements

The authors would like to acknowledge the following individuals for their contributions to this manuscript: Dr. R. Brad Jones for providing the OM9 B LCLs; Dr. Michael Keller at Children's National Hospital in Washington, DC for providing the HLA-B*35-restricted pp65 peptide; Dr. Catherine Bollard for providing the non-OM9 B LCLs; Dr. Gregory Cresswell for assistance with flow cytometry data analysis; all blood donors; all patients.

Authors' contributions

Conceptualization: EEG, DJP, RBJ, CRYC, CBM, KBC Data curation: EEG Formal Analysis: EEG, HGD Funding acquisition: EEG, CRYC, KBC Investigation: EEG, LCS, LW, AVL Methodology: EEG, LCS, CRYC, HGD Project administration: EEG, KBC Resources: LCS, DJP, RBJ, MO, KBC, NPC, JCA Software: EEG Supervision: DJP, CBM, CRYC, KBC Validation: EEG, KBC Visualization: EEG, KBC Writing – original draft: EEG, KBC Writing – review & editing: EEG, LS, CRYC, DJP, KBC.

Funding

Research was supported by the National Cancer Institute R00CA204592 and R37CA251270 (to KBC), the DOD Ovarian Cancer Research Program (W81XWH2010273 to KBC), and by the Marlene and Michael Berman Endowed Fund for Ovarian Cancer Research. EEG was supported by a NRSA Predoctoral Fellowship (NIH/NCI 1F31CA271788) and The Cosmos Scholars Grant Program. The authors would like to acknowledge the Integrated for Biomedical Sciences at the George Washington University for graduate student support and training (EEG). The funding sources listed had no involvement in or influence on: the study design; data collection or interpretation; or the writing, preparation, or decision to submit this manuscript for publication.

Availability of data and materials

Data is provided within the manuscript and supplementary information files.

Declarations

Ethics approval and consent to participate

PBMCs and ascites samples were obtained with informed consent from patients at the GW University Hospital in Washington, DC in accordance with Institutional Review Board protocol #180205. All blood donors gave informed consent prior to donating.

Consent for publication

Not applicable to this study.

Competing interests

KBC is a consultant for Rome Therapeutics.

Received: 16 May 2024 Accepted: 4 October 2024
Published online: 09 October 2024

References

1. Zhang R, Siu MKY, Ngan HYS, Chan KKL. Molecular Biomarkers for the Early Detection of Ovarian Cancer. Int J Mol Sci. 2022;23:12041. https://doi.org/10.3390/ijms231912041.
2. Narod S. Can Advanced-Stage Ovarian Cancer Be Cured? Nat Rev Clin Oncol. 2016;13:255–61. https://doi.org/10.1038/nrclinonc.2015.224.
3. Rizvi, N.A.; Hellmann, M.D.; Snyder, A.; Kvistborg, P.; Makarov, V.; Havel, J.J.; Lee, W.; Yuan, J.; Wong, P.; Ho, T.S.; et al. Cancer Immunology. Mutational Landscape Determines Sensitivity to PD-1 Blockade in Non-Small Cell Lung Cancer. Science 2015;348:124–128. https://doi.org/10.1126/science.aaa1348.
4. Desrichard A, Snyder A, Chan TA. Cancer Neoantigens and Applications for Immunotherapy. Clin Cancer Res. 2016;22:807–12. https://doi.org/10.1158/1078-0432.CCR-14-3175.
5. Schumacher TN, Schreiber RD. Neoantigens in Cancer Immunotherapy. Science. 2015;348:69–74. https://doi.org/10.1126/science.aaa4971.
6. Hamanishi J, Mandai M, Ikeda T, Minami M, Kawaguchi A, Murayama T, Kanai M, Mori Y, Matsumoto S, Chikuma S, et al. Safety and Antitumor Activity of Anti-PD-1 Antibody, Nivolumab, in Patients With

Platinum-Resistant Ovarian Cancer. J Clin Oncol Off J Am Soc Clin Oncol. 2015;33:4015–22. https://doi.org/10.1200/JCO.2015.62.3397.
7. Disis ML, Taylor MH, Kelly K, Beck JT, Gordon M, Moore KM, Patel MR, Chaves J, Park H, Mita AC, et al. Efficacy and Safety of Avelumab for Patients With Recurrent or Refractory Ovarian Cancer: Phase 1b Results From the JAVELIN Solid Tumor Trial. JAMA Oncol. 2019;5:393–401. https://doi.org/10.1001/jamaoncol.2018.6258.
8. Liu JF, Gordon M, Veneris J, Braiteh F, Balmanoukian A, Eder JP, Oaknin A, Hamilton E, Wang Y, Sarkar I, et al. Safety, Clinical Activity and Biomarker Assessments of Atezolizumab from a Phase I Study in Advanced/Recurrent Ovarian and Uterine Cancers. Gynecol Oncol. 2019;154:314–22. https://doi.org/10.1016/j.ygyno.2019.05.021.
9. Zamarin D, Burger RA, Sill MW, Powell DJ, Lankes HA, Feldman MD, Zivanovic O, Gunderson C, Ko E, Mathews C, et al. Randomized Phase II Trial of Nivolumab Versus Nivolumab and Ipilimumab for Recurrent or Persistent Ovarian Cancer: An NRG Oncology Study. J Clin Oncol Off J Am Soc Clin Oncol. 2020;38:1814–23. https://doi.org/10.1200/JCO.19.02059.
10. Chardin, L.; Leary, A. Immunotherapy in Ovarian Cancer: Thinking Beyond PD-1/PD-L1. Front. Oncol. 2021;11. https://doi.org/10.3389/fonc.2021.795547.
11. Monk BJ, Colombo N, Oza AM, Fujiwara K, Birrer MJ, Randall L, Poddubskaya EV, Scambia G, Shparyk YV, Lim MC, et al. Chemotherapy with or without Avelumab Followed by Avelumab Maintenance versus Chemotherapy Alone in Patients with Previously Untreated Epithelial Ovarian Cancer (JAVELIN Ovarian 100): An Open-Label, Randomised, Phase 3 Trial. Lancet Oncol. 2021;22:1275–89. https://doi.org/10.1016/S1470-2045(21)00342-9.
12. Pujade-Lauraine E, Fujiwara K, Ledermann JA, Oza AM, Kristeleit R, Ray-Coquard I-L, Richardson GE, Sessa C, Yonemori K, Banerjee S, et al. Avelumab Alone or in Combination with Chemotherapy versus Chemotherapy Alone in Platinum-Resistant or Platinum-Refractory Ovarian Cancer (JAVELIN Ovarian 200): An Open-Label, Three-Arm, Randomised, Phase 3 Study. Lancet Oncol. 2021;22:1034–46. https://doi.org/10.1016/S1470-2045(21)00216-3.
13. Moore KN, Bookman M, Sehouli J, Miller A, Anderson C, Scambia G, Myers T, Taskiran C, Robison K, Mäenpää J, et al. Atezolizumab, Bevacizumab, and Chemotherapy for Newly Diagnosed Stage III or IV Ovarian Cancer: Placebo-Controlled Randomized Phase III Trial (IMagyn050/GOG 3015/ENGOT-OV39). J Clin Oncol Off J Am Soc Clin Oncol. 2021;39:1842–55. https://doi.org/10.1200/JCO.21.00306.
14. Kurtz J-E, Pujade-Lauraine E, Oaknin A, Belin L, Leitner K, Cibula D, Denys H, Rosengarten O, Rodrigues M, de Gregorio N, et al. Atezolizumab Combined With Bevacizumab and Platinum-Based Therapy for Platinum-Sensitive Ovarian Cancer: Placebo-Controlled Randomized Phase III ATALANTE/ENGOT-Ov29 Trial. J Clin Oncol Off J Am Soc Clin Oncol. 2023;41:4768–78. https://doi.org/10.1200/JCO.23.00529.
15. Chiappinelli KB, Strissel PL, Desrichard A, Li H, Henke C, Akman B, Hein A, Rote NS, Cope LM, Snyder A, et al. Inhibiting DNA Methylation Causes an Interferon Response in Cancer via dsRNA Including Endogenous Retroviruses. Cell. 2015;162:974–86. https://doi.org/10.1016/j.cell.2015.07.011.
16. Stone ML, Chiappinelli KB, Li H, Murphy LM, Travers ME, Topper MJ, Mathios D, Lim M, Shih I-M, Wang T-L, et al. Epigenetic Therapy Activates Type I Interferon Signaling in Murine Ovarian Cancer to Reduce Immunosuppression and Tumor Burden. Proc Natl Acad Sci U S A. 2017;114:E10981–90. https://doi.org/10.1073/pnas.1712514114.
17. Gomez S, Cox OL, Walker RR, Rentia U, Hadley M, Arthofer E, Diab N, Grundy EE, Kanholm T, McDonald JI, et al. Inhibiting DNA Methylation and RNA Editing Upregulates Immunogenic RNA to Transform the Tumor Microenvironment and Prolong Survival in Ovarian Cancer. J Immunother Cancer. 2022;10:e004974. https://doi.org/10.1136/jitc-2022-004974.
18. Pappalardo XG, Barra V. Losing DNA Methylation at Repetitive Elements and Breaking Bad. Epigenetics Chromatin. 2021;14:25. https://doi.org/10.1186/s13072-021-00400-z.
19. Grundy EE, Diab N, Chiappinelli KB. Transposable Element Regulation and Expression in Cancer. FEBS J. 2022;289:1160–79. https://doi.org/10.1111/febs.15722.
20. Roulois D, Loo Yau H, Singhania R, Wang Y, Danesh A, Shen SY, Han H, Liang G, Jones PA, Pugh TJ, et al. DNA-Demethylating Agents Target Colorectal Cancer Cells by Inducing Viral Mimicry by Endogenous Transcripts. Cell. 2015;162:961–73. https://doi.org/10.1016/j.cell.2015.07.056.
21. Wrangle J, Wang W, Koch A, Easwaran H, Mohammad HP, Vendetti F, VanCriekinge W, DeMeyer T, Du Z, Parsana P, et al. Alterations of Immune Response of Non-Small Cell Lung Cancer with Azacytidine. Oncotarget. 2013;4:2067–79. https://doi.org/10.18632/oncotarget.1542.
22. Li H, Chiappinelli KB, Guzzetta AA, Easwaran H, Yen R-WC, Vatapalli R, Topper MJ, Luo J, Connolly RM, Azad NS, et al. Immune Regulation by Low Doses of the DNA Methyltransferase Inhibitor 5-Azacitidine in Common Human Epithelial Cancers. Oncotarget. 2014;5:587–98. https://doi.org/10.18632/oncotarget.1782.
23. Zhang L, Conejo-Garcia JR, Katsaros D, Gimotty PA, Massobrio M, Regnani G, Makrigiannakis A, Gray H, Schlienger K, Liebman MN, et al. Intratumoral T Cells, Recurrence, and Survival in Epithelial Ovarian Cancer. N Engl J Med. 2003;348:203–13. https://doi.org/10.1056/NEJMoa020177.
24. Sato E, Olson SH, Ahn J, Bundy B, Nishikawa H, Qian F, Jungbluth AA, Frosina D, Gnjatic S, Ambrosone C, et al. Intraepithelial CD8+ Tumor-Infiltrating Lymphocytes and a High CD8+/Regulatory T Cell Ratio Are Associated with Favorable Prognosis in Ovarian Cancer. Proc Natl Acad Sci U S A. 2005;102:18538–43. https://doi.org/10.1073/pnas.0509182102.
25. Kroeger PT, Drapkin R. Pathogenesis and Heterogeneity of Ovarian Cancer. Curr Opin Obstet Gynecol. 2017;29:26–34. https://doi.org/10.1097/GCO.0000000000000340.
26. Shih I-M, Wang Y, Wang T-L. The Origin of Ovarian Cancer Species and Precancerous Landscape. Am J Pathol. 2021;191:26–39. https://doi.org/10.1016/j.ajpath.2020.09.006.
27. Wang-Johanning F, Liu J, Rycaj K, Huang M, Tsai K, Rosen DG, Chen D-T, Lu DW, Barnhart KF, Johanning GL. Expression of Multiple Human Endogenous Retrovirus Surface Envelope Proteins in Ovarian Cancer. Int J Cancer. 2007;120:81–90. https://doi.org/10.1002/ijc.22256.
28. Natoli M, Gallon J, Lu H, Amgheib A, Pinato DJ, Mauri FA, Marafioti T, Akarca AU, Ullmo I, Ip J, et al. Transcriptional Analysis of Multiple Ovarian Cancer Cohorts Reveals Prognostic and Immunomodulatory Consequences of ERV Expression. J Immunother Cancer. 2021;9:e001519. https://doi.org/10.1136/jitc-2020-001519.
29. Rycaj, K.; Plummer, J.B.; Yin, B.; Li, M.; Garza, J.; Radvanyi, L.; Ramondetta, L.M.; Lin, K.; Johanning, G.L.; Tang, D.G.; et al. Cytotoxicity of Human Endogenous Retrovirus K-Specific T Cells toward Autologous Ovarian Cancer Cells. Clin. Cancer Res. Off. J. Am. Assoc. Cancer Res. 2015;21:471–483. https://doi.org/10.1158/1078-0432.CCR-14-0388.
30. Lander ES, Linton LM, Birren B, Nusbaum C, Zody MC, Baldwin J, Devon K, Dewar K, Doyle M, FitzHugh W, et al. Initial Sequencing and Analysis of the Human Genome. Nature. 2001;409:860–921. https://doi.org/10.1038/35057062.
31. Blomberg J, Benachenhou F, Blikstad V, Sperber G, Mayer J. Classification and Nomenclature of Endogenous Retroviral Sequences (ERVs): Problems and Recommendations. Gene. 2009;448:115–23. https://doi.org/10.1016/j.gene.2009.06.007.
32. Löwer R, Löwer J, Kurth R. The Viruses in All of Us: Characteristics and Biological Significance of Human Endogenous Retrovirus Sequences. Proc Natl Acad Sci U S A. 1996;93:5177–84.
33. Büscher K, Trefzer U, Hofmann M, Sterry W, Kurth R, Denner J. Expression of Human Endogenous Retrovirus K in Melanomas and Melanoma Cell Lines. Cancer Res. 2005;65:4172–80. https://doi.org/10.1158/0008-5472.CAN-04-2983.
34. Serafino A, Balestrieri E, Pierimarchi P, Matteucci C, Moroni G, Oricchio E, Rasi G, Mastino A, Spadafora C, Garaci E, et al. The Activation of Human Endogenous Retrovirus K (HERV-K) Is Implicated in Melanoma Cell Malignant Transformation. Exp Cell Res. 2009;315:849–62. https://doi.org/10.1016/j.yexcr.2008.12.023.
35. Schanab O, Humer J, Gleiss A, Mikula M, Sturlan S, Grunt S, Okamoto I, Muster T, Pehamberger H, Waltenberger A. Expression of Human Endogenous Retrovirus K Is Stimulated by Ultraviolet Radiation in Melanoma. Pigment Cell Melanoma Res. 2011;24:656–65. https://doi.org/10.1111/j.1755-148X.2011.00860.x.
36. Reis, B.S.; Jungbluth, A.A.; Frosina, D.; Holz, M.; Ritter, E.; Nakayama, E.; Ishida, T.; Obata, Y.; Carver, B.; Scher, H.; et al. Prostate Cancer Progression Correlates with Increased Humoral Immune Response to a Human Endogenous Retrovirus GAG Protein. Clin. Cancer Res. Off. J. Am. Assoc. Cancer Res. 2013, 19, 6112–6125, https://doi.org/10.1158/1078-0432.CCR-12-3580.
37. Li, M.; Radvanyi, L.; Yin, B.; Rycaj, K.; Li, J.; Chivukula, R.; Lin, K.; Lu, Y.; Shen, J.; Chang, D.Z.; et al. Downregulation of Human Endogenous Retrovirus

Type K (HERV-K) Viral Env RNA in Pancreatic Cancer Cells Decreases Cell Proliferation and Tumor Growth. Clin. Cancer Res. Off. J. Am. Assoc. Cancer Res. 2017;23:5892–5911. https://doi.org/10.1158/1078-0432.CCR-17-0001.
38. Jones RB, Garrison KE, Mujib S, Mihajlovic V, Aidarus N, Hunter DV, Martin E, John VM, Zhan W, Faruk NF, et al. HERV-K-Specific T Cells Eliminate Diverse HIV-1/2 and SIV Primary Isolates. J Clin Invest. 2012;122:4473–89. https://doi.org/10.1172/JCI64560.
39. Nadeau M-J, Manghera M, Douville RN. Inside the Envelope: Endogenous Retrovirus-K Env as a Biomarker and Therapeutic Target. Front Microbiol. 2015;6:1244. https://doi.org/10.3389/fmicb.2015.01244.
40. ERVK-6 - Endogenous Retrovirus Group K Member 6 Env Polyprotein - Homo Sapiens (Human) | UniProtKB | UniProt Available online: https://www.uniprot.org/uniprotkb/Q69384/entry (accessed on 9 August 2023).
41. Rossjohn J, Gras S, Miles JJ, Turner SJ, Godfrey DI, McCluskey J. T Cell Antigen Receptor Recognition of Antigen-Presenting Molecules. Annu Rev Immunol. 2015;33:169–200. https://doi.org/10.1146/annurev-immunol-032414-112334.
42. Trolle T, McMurtrey CP, Sidney J, Bardet W, Osborn SC, Kaever T, Sette A, Hildebrand WH, Nielsen M, Peters B. The Length Distribution of Class I Restricted T Cell Epitopes Is Determined by Both Peptide Supply and MHC Allele Specific Binding Preference. J Immunol Baltim Md. 1950;2016(196):1480–7. https://doi.org/10.4049/jimmunol.1501721.
43. The Allele Frequency Net Database [Search HLA Haplotype Frequencies] Available online: http://www.allelefrequencies.net/hla6003a.asp?hla_locus1=A*03%3A01&hla_locus2=&hla_locus3=&hla_locus4=&hla_locus5=&hla_locus6=&hla_locus7=&hla_locus8=&hla_population=&hla_country=&hla_dataset=&hla_region=North+America&hla_ethnic=&hla_study=&hla_order=order_1&hla_sample_size_pattern=equal&hla_sample_size=&hla_sample_year_pattern=equal&hla_sample_year=&hla_loci= (accessed on 17 August 2023).
44. Chilson OP, Boylston AW, Crumpton MJ. Phaseolus Vulgaris Phytohaemagglutinin (PHA) Binds to the Human T Lymphocyte Antigen Receptor. EMBO J. 1984;3:3239–45. https://doi.org/10.1002/j.1460-2075.1984.tb02285.x.
45. Ngo MC, Ando J, Leen AM, Ennamuri S, Lapteva N, Vera JF, Min-Venditti A, Mims MP, Heslop HE, Bollard CM, et al. Complementation of Antigen Presenting Cells to Generate T Lymphocytes with Broad Target Specificity. J Immunother Hagerstown Md. 1997;2014(37):193–203. https://doi.org/10.1097/CJI.0000000000000014.
46. Bollard CM, Aguilar L, Straathof KC, Gahn B, Huls MH, Rousseau A, Sixbey J, Gresik MV, Carrum G, Hudson M, et al. Cytotoxic T Lymphocyte Therapy for Epstein-Barr Virus+ Hodgkin's Disease. J Exp Med. 2004;200:1623–33. https://doi.org/10.1084/jem.20040890.
47. Durkee-Shock J, Lazarski CA, Jensen-Wachspress MA, Zhang A, Son A, Kankate VV, Field NE, Webber K, Lang H, Conway SR, et al. Transcriptomic Analysis Reveals Optimal Cytokine Combinations for SARS-CoV-2-Specific T Cell Therapy Products. Mol Ther Methods Clin Dev. 2022;25:439–47. https://doi.org/10.1016/j.omtm.2022.04.013.
48. Hanajiri R, Sani GM, Hanley PJ, Silveira CG, Kallas EG, Keller MD, Bollard CM. Generation of Zika Virus-Specific T-Cells from Seropositive and Virus Naïve Donors for Potential Use as an Autologous or "Off the Shelf" Immunotherapeutic. Cytotherapy. 2019;21:840–55. https://doi.org/10.1016/j.jcyt.2019.06.008.
49. Calarota SA, Baldanti F. Enumeration and Characterization of Human Memory T Cells by Enzyme-Linked Immunospot Assays. Clin Dev Immunol. 2013;2013:637649. https://doi.org/10.1155/2013/637649.
50. Boegel S, Löwer M, Bukur T, Sahin U, Castle JC. A Catalog of HLA Type, HLA Expression, and Neo-Epitope Candidates in Human Cancer Cell Lines. Oncoimmunology. 2014;3:e954893. https://doi.org/10.4161/21624011.2014.954893.
51. Lange, P.T.; Damania, B. Epstein-Barr Virus-Positive Lymphomas Exploit Ectonucleotidase Activity To Limit Immune Responses and Prevent Cell Death. mBio .2023;14:e0345922. https://doi.org/10.1128/mbio.03459-22.
52. Yang J, Lemas VM, Flinn IW, Krone C, Ambinder RF. Application of the ELISPOT Assay to the Characterization of CD8+ Responses to Epstein-Barr Virus Antigens. Blood. 2000;95:241–8. https://doi.org/10.1182/blood.V95.1.241.
53. Pender MP, Csurhes PA, Lenarczyk A, Pfluger CMM, Burrows SR. Decreased T Cell Reactivity to Epstein-Barr Virus Infected Lymphoblastoid Cell Lines in Multiple Sclerosis. J Neurol Neurosurg Psychiatry. 2009;80:498–505. https://doi.org/10.1136/jnnp.2008.161018.
54. Lakkis FG, Lechler RI. Origin and Biology of the Allogeneic Response. Cold Spring Harb Perspect Med. 2013;3:a014993. https://doi.org/10.1101/cshperspect.a014993.
55. Molvi Z. Activation of Human T Cells with Phytohaemagglutinin (PHA) V1; 2020. https://doi.org/10.17504/protocols.io.bpigmkbw.
56. Weber, G.; Gerdemann, U.; Caruana, I.; Savoldo, B.; Hensel, N.; Rabin, K.; Shpall, E.; Melenhorst, J.; Leen, A.; Barrett, A.; et al. Generation of Multi-Leukemia Antigen-Specific T Cells to Enhance the Graft-versus-Leukemia Effect after Allogeneic Stem Cell Transplant. Leukemia 2013;27. https://doi.org/10.1038/leu.2013.66, https://doi.org/10.1038/leu.2013.66.
57. Varma TK, Lin CY, Toliver-Kinsky TE, Sherwood ER. Endotoxin-Induced Gamma Interferon Production: Contributing Cell Types and Key Regulatory Factors. Clin Diagn Lab Immunol. 2002;9:530–43. https://doi.org/10.1128/CDLI.9.3.530-543.2002.
58. van Baren N, Chambost H, Ferrant A, Michaux L, Ikeda H, Millard I, Olive D, Boon T, Coulie PG. PRAME, a Gene Encoding an Antigen Recognized on a Human Melanoma by Cytolytic T Cells, Is Expressed in Acute Leukaemia Cells. Br J Haematol. 1998;102:1376–9. https://doi.org/10.1046/j.1365-2141.1998.00982.x.
59. Stanojevic M, Hont AB, Geiger A, O'Brien S, Ulrey R, Grant M, Datar A, Lee P-H, Lang H, Cruz CRY, et al. Identification of Novel HLA-Restricted Preferentially Expressed Antigen in Melanoma Peptides to Facilitate off-the-Shelf Tumor-Associated Antigen-Specific T-Cell Therapies. Cytotherapy. 2021;23:694–703. https://doi.org/10.1016/j.jcyt.2021.03.001.
60. Bullock TNJ, Colella TA, Engelhard VH. The Density of Peptides Displayed by Dendritic Cells Affects Immune Responses to Human Tyrosinase and Gp100 in HLA-A2 Transgenic Mice1. J Immunol. 2000;164:2354–61. https://doi.org/10.4049/jimmunol.164.5.2354.
61. Sallusto F, Lenig D, Förster R, Lipp M, Lanzavecchia A. Two Subsets of Memory T Lymphocytes with Distinct Homing Potentials and Effector Functions. Nature. 1999;401:708–12. https://doi.org/10.1038/44385.
62. Kaech SM, Ahmed R. Memory CD8+ T Cell Differentiation: Initial Antigen Encounter Triggers a Developmental Program in Naïve Cells. Nat Immunol. 2001;2:415–22. https://doi.org/10.1038/87720.
63. Principe, N.; Kidman, J.; Goh, S.; Tilsed, C.M.; Fisher, S.A.; Fear, V.S.; Forbes, C.A.; Zemek, R.M.; Chopra, A.; Watson, M.; et al. Tumor Infiltrating Effector Memory Antigen-Specific CD8+ T Cells Predict Response to Immune Checkpoint Therapy. Front. Immunol. 2020;11. https://doi.org/10.3389/fimmu.2020.584423.
64. Weber, G.; Caruana, I.; Rouce, R.H.; Barrett, A.J.; Gerdemann, U.; Leen, A.M.; Rabin, K.R.; Bollard, C.M. Generation of Tumor Antigen-Specific T Cell Lines from Pediatric Patients with Acute Lymphoblastic Leukemia--Implications for Immunotherapy. Clin. Cancer Res. Off. J. Am. Assoc. Cancer Res. 2013;19:5079–5091. https://doi.org/10.1158/1078-0432.CCR-13-0955.
65. Wang-Johanning F, Radvanyi L, Rycaj K, Plummer JB, Yan P, Sastry KJ, Piyathilake CJ, Hunt KK, Johanning GL. Human Endogenous Retrovirus K Triggers an Antigen-Specific Immune Response in Breast Cancer Patients. Cancer Res. 2008;68:5869–77. https://doi.org/10.1158/0008-5472.CAN-07-6838.
66. Stanojevic M, Geiger A, Ostermeier B, Sohai D, Lazarski C, Lang H, Jensen-Wachspress M, Webber K, Burbelo P, Cohen J, et al. Spike-Directed Vaccination Elicits Robust Spike-Specific T-Cell Response. Including to Mutant Strains Cytotherapy. 2022;24:10–5. https://doi.org/10.1016/j.jcyt.2021.07.006.
67. Wölfl M, Greenberg PD. Antigen-Specific Activation and Cytokine-Facilitated Expansion of Naive, Human CD8+ T Cells. Nat Protoc. 2014;9:950–66. https://doi.org/10.1038/nprot.2014.064.
68. Alcazer V, Bonaventura P, Tonon L, Michel E, Mutez V, Fabres C, Chuvin N, Boulos R, Estornes Y, Maguer-Satta V, et al. HERVs Characterize Normal and Leukemia Stem Cells and Represent a Source of Shared Epitopes for Cancer Immunotherapy. Am J Hematol. 2022;97:1200–14. https://doi.org/10.1002/ajh.26647.
69. Bonaventura, P.; Alcazer, V.; Mutez, V.; Tonon, L.; Martin, J.; Chuvin, N.; Michel, E.; Boulos, R.E.; Estornes, Y.; Valladeau-Guilemond, J.; et al. Identification of Shared Tumor Epitopes from Endogenous Retroviruses Inducing High-Avidity Cytotoxic T Cells for Cancer Immunotherapy. Sci. Adv. 2022;8:eabj3671. https://doi.org/10.1126/sciadv.abj3671.
70. Shah NM, Jang HJ, Liang Y, Maeng JH, Tzeng S-C, Wu A, Basri NL, Qu X, Fan C, Li A, et al. Pan-Cancer Analysis Identifies Tumor-Specific Antigens Derived from Transposable Elements. Nat Genet. 2023;55:631–9. https://doi.org/10.1038/s41588-023-01349-3.

71. Bonté P-E, Arribas YA, Merlotti A, Carrascal M, Zhang JV, Zueva E, Binder ZA, Alanio C, Goudot C, Amigorena S. Single-Cell RNA-Seq-Based Proteogenomics Identifies Glioblastoma-Specific Transposable Elements Encoding HLA-I-Presented Peptides. Cell Rep. 2022;39:110916. https://doi.org/10.1016/j.celrep.2022.110916.
72. Kong Y, Rose CM, Cass AA, Williams AG, Darwish M, Lianoglou S, Haverty PM, Tong A-J, Blanchette C, Albert ML, et al. Transposable Element Expression in Tumors Is Associated with Immune Infiltration and Increased Antigenicity. Nat Commun. 2019;10:5228. https://doi.org/10.1038/s41467-019-13035-2.
73. Burbage, M.; Rocañín-Arjó, A.; Baudon, B.; Arribas, Y.A.; Merlotti, A.; Rookhuizen, D.C.; Heurtebise-Chrétien, S.; Ye, M.; Houy, A.; Burgdorf, N.; et al. Epigenetically Controlled Tumor Antigens Derived from Splice Junctions between Exons and Transposable Elements. Sci. Immunol. 2023;8:eabm6360. https://doi.org/10.1126/sciimmunol.abm6360.
74. Barisic S, Brahmbhatt EM, Cherkasova E, Spear TT, Savani U, Pierre S, Scurti GM, Chen L, Igboko M, Nadal R, et al. Regression of Renal Cell Carcinoma by T Cell Receptor-Engineered T Cells Targeting a Human Endogenous Retrovirus. J Immunother Cancer. 2024;12:e009147. https://doi.org/10.1136/jitc-2024-009147.
75. Nadal R, Barisic S, Scurti GM, Cherkasova E, Chen L, Wood K, Highfill SL, Wells B, Aue G, Shalabi R, et al. Phase I Results of Human Endogenous Retrovirus Type-E (HERV-E) TCR Transduced T-Cells in Patients (Pts) with Metastatic Clear Cell Renal Cell Carcinoma (mccRCC). J Clin Oncol. 2023;41:2549–2549. https://doi.org/10.1200/JCO.2023.41.16_suppl.2549.
76. Tosato, G.; Cohen, J.I. Generation of Epstein-Barr Virus (EBV)–Immortalized B Cell Lines. Curr. Protoc. Immunol. 2007;76:7.22.1–7.22.4. https://doi.org/10.1002/0471142735.im0722s76.
77. McCormack SE, Cruz CRY, Wright KE, Powell AB, Lang H, Trimble C, Keller MD, Fuchs E, Bollard CM. Human Papilloma Virus-Specific T Cells Can Be Generated from Naïve T Cells for Use as an Immunotherapeutic Strategy for Immunocompromised Patients. Cytotherapy. 2018;20:385–93. https://doi.org/10.1016/j.jcyt.2017.11.010.
78. Sweeney EE, Sekhri P, Telaraja D, Chen J, Chin SJ, Chiappinelli KB, Sanchez CE, Bollard CM, Cruz CRY, Fernandes R. Engineered Tumor-Specific T Cells Using Immunostimulatory Photothermal Nanoparticles. Cytotherapy. 2023;25:718–27. https://doi.org/10.1016/j.jcyt.2023.03.014.

Publisher's Note